

Quantum Graph Drawing

Susanna Caroppo, Giordano Da Lozzo, and Giuseppe Di Battista

Roma Tre University

{susanna.caroppo,giordano.dalozzo,giuseppe.dibattista}@uniroma3.it

Abstract

In this paper, we initiate the study of quantum algorithms in the Graph Drawing research area. We focus on two foundational drawing standards: *2-level drawings* and *book layouts*. Concerning 2-level drawings, we consider the problems of obtaining drawings with the minimum number of crossings, k -planar drawings, quasi-planar drawings, and the problem of removing the minimum number of edges to obtain a 2-level planar graph. Concerning book layouts, we consider the problems of obtaining 1-page book layouts with the minimum number of crossings, book embeddings with the minimum number of pages, and the problem of removing the minimum number of edges to obtain an outerplanar graph. We explore both the quantum circuit and the quantum annealing models of computation. In the *quantum circuit model*, we provide an algorithmic framework based on Grover's quantum search, which allows us to obtain, at least, a quadratic speedup on the best classical exact algorithms for all the considered problems. In the *quantum annealing model*, we perform experiments on the quantum processing unit provided by D-Wave, focusing on the classical 2-level crossing minimization problem, demonstrating that quantum annealing is competitive with respect to classical algorithms.

Keywords: Quantum complexity, Grover's algorithm, QUBO, D-Wave, 2-Level drawings, Book layouts

Contents

1	Introduction	3
2	Preliminaries	5
3	Basic Quantum Circuits	7
4	A Quantum Framework for Graph Drawing Problems	12
5	Input Transducer Circuits	14
5.1	Order Transducer	14
5.2	Skewness Transducer	16
6	Solution Detector Circuits	17
6.1	Problem TLCM	18
6.2	Problem TLKP	20
6.3	Problem TLQP	22
6.4	Problem TLS	24
6.5	Problem OPCM	26
6.6	Problem BT	28
6.7	Problem BS	30
7	Exploiting Quantum Annealing for Graph Drawing	31
7.1	CBO Formulations for Two-Level Problems	31
7.2	CBO Formulations for Book-layout problems	32
7.3	From CBO to QUBO	33
7.4	D-Wave Experimentation	34
8	Conclusions and Open Problems	34

1 Introduction

In this paper, we initiate the study of quantum algorithms in the Graph Drawing research area. We focus on two foundational graph drawing standards: *2-level drawings* and *book layouts*. In a *2-level drawing*, the graph is bipartite, the vertices are placed on two horizontal lines, and the edges are drawn as y -monotone curves. In this drawing standard, we consider the search version of the **TWO-LEVEL CROSSING MINIMIZATION** (TLCM) problem, where given an integer ρ we seek a 2-level drawing with at most ρ crossings, and of the **TWO-LEVEL SKEWNESS** (TLS) problem, where given an integer σ we seek to determine a set of σ edges whose removal yields a *2-level planar graph*, i.e., a forest of caterpillars [11]. The minimum value of σ is the *2-level skewness* of the considered graph. We also consider the **TWO-LEVEL QUASI PLANARITY** (TLQP) problem, where we seek a drawing in which no three edges pairwise cross, i.e., a *quasi-planar* drawing, and the **TWO-LEVEL k -PLANARITY** (TLKP) problem, where we seek a drawing in which each edge participates to at most k crossings, i.e., a *k -planar* drawing. In a *book layout*, the drawing is constructed using a collection of half-planes, called *pages*, all having the same line, called *spine*, as their boundary. The vertices lie on the spine and each edge is drawn on a page. In this drawing standard, we consider the search version of the **ONE-PAGE CROSSING MINIMIZATION** (OPCM) problem, where given an integer ρ we seek a 1-page layout with at most ρ crossings; the **BOOK THICKNESS** (BT) problem, where we search a τ -page layout where the edges in the same page do not cross, i.e., a *τ -page book embedding*; and the **BOOK SKEWNESS** (BS) problem, where given an integer σ we seek a set of σ edges whose removal yields a graph admitting a *1-page book embedding*, i.e., it is outerplanar [5]. The minimum value of σ is the *book skewness* of the considered graph.

Our contributions. We delve into both the *quantum circuit* [21, 23] and the *quantum annealing* [20] models of computation. In the former, quantum gates are used to compose a circuit that transforms an input superposition of qubits into an output superposition. The circuit design depends on both the problem and the specific instance being processed. The output superposition is eventually measured, obtaining the solution with a certain probability. The quality of the circuit is measured in terms of its *circuit complexity*, which is the number of elementary gates it contains, of its *depth*, which is the maximum number of a chain of elementary gates from the input to the output, and of its *width*, which is the maximum number of elementary gates “along a cut” separating the input from the output. It is natural to upper bound the time complexity of the execution of a quantum circuit either by its depth, assuming the gates at each layer can be executed in parallel, or by its circuit complexity, assuming the gates are executed sequentially. The width estimates the desired level of parallelism. In the latter, quantum annealing processors, in general quite different from those designed for the quantum circuit model, consist of a fixed-topology network, whose vertices correspond to qubits and whose edges correspond to possible interactions between qubits. A problem is mapped to an embedding on such a topology. During the computation, the solution space of a problem is explored, searching for minimum-energy states, which correspond to, in general approximate, solutions.

In the quantum circuit model, we first show that the above graph drawing problems can be described by means of quantum circuits. To do that, we introduce several efficient elementary circuits, that can be of general usage in *Quantum Graph Drawing*. Second, we present an algorithmic framework based on Grover’s quantum search approach. This framework enables us to achieve, at least, a quadratic speedup compared to the best exact classical algorithms for all the problems under consideration. Table 1 overviews our complexity results and compares them with exact algorithms.

In the quantum annealing model, we focus on the processing unit provided by D-Wave, which allows us to perform *hybrid computations*, i.e., computations that are partly classical and partly quantum. We first show that it is relatively easy to use D-Wave for implementing heuristics for the above problems. Second, we focus on the classical TLCM problem. Through experiments, we demonstrate that quantum annealing exhibits competitiveness when compared to classical algorithms. Table 2 overviews our experimental findings.

State of the art. We now provide an overview of the complexity status of each of the considered problems, together with the existence of FPT algorithms with respect to the corresponding natural parameter (total number of crossings ρ , number of crossings per edge k , maximum number of allowed mutually crossing edges, number of pages τ , and number of edges to be removed σ), density bounds, and exact algorithms. Let n and m denote the number of vertices and edges of an input graph, respectively.

TLCM is probably the most studied among the above problems (see, e.g., [10, 16]). It is NP-complete [13], and it remains NP-complete even when the order on one level is prescribed [12]. Kobayashi

Table 1: Results presented in this paper and comparison with exact algorithms. FPT algorithms are mentioned, if any, only with respect to the natural parameter. CC stands for Circuit Complexity. M denotes the number of solutions to the considered problem.

Problem	Classic Algorithm Running Time	Upperbound for m	FPT Time	Quantum Oracle Calls	Oracles (Lemma 4.2)		
					CC	Depth	Width
TLCM	$2^{n \log n} O(m^2)$	$O(\sqrt[3]{\rho \cdot n^2})$ [3]	$2^{O(\rho)} + n^{O(1)}$ [18]	$\frac{\pi}{4} \sqrt{\frac{2^{n \log n}}{M}}$	$O(m^2)$	$O(n^2)$	$O(m^2)$
TLKP	$2^{n \log n} O(m^2)$	$O(\sqrt{k} \cdot n)$ [3]	-	$\frac{\pi}{4} \sqrt{\frac{2^{n \log n}}{M}}$	$O(m^2)$	$O(m \log^2 m)$	$O(m)$
TLQP	$2^{n \log n} O(m^3)$	$O(n)$ [3]	Para-NP-hard [2]	$\frac{\pi}{4} \sqrt{\frac{2^{n \log n}}{M}}$	$O(m^6)$	$O(m^4)$	$O(m^2)$
TLS	$O(m^\sigma n)$	$O(n + \sigma)$	$2^{O(\sigma^3)} n$ [10]	$\frac{\pi}{4} \sqrt{\frac{2^{n \log n + \sigma \log m}}{M}}$	$O(m^2)$	$O(m)$	$O(m)$
OPCM	$2^{n \log n} O(m^2)$	$O(\sqrt[3]{\rho \cdot n^2})$ [24]	Courcelle's Th. [4]	$\frac{\pi}{4} \sqrt{\frac{2^{n \log n}}{M}}$	$O(n^8)$	$O(n^6)$	$O(m^2)$
BT	$2^{n \log n + m \log \tau} O(\tau n)$	$O(\tau \cdot n)$	Para-NP-hard [19]	$\frac{\pi}{4} \sqrt{\frac{2^{n \log n + m \log \tau}}{M}}$	$O(n^8)$	$O(n^6)$	$O(m)$
BS	$O(m^\sigma n)$	$O(n + \sigma)$	-	$\frac{\pi}{4} \sqrt{\frac{2^{n \log n + \sigma \log m}}{M}}$	$O(n^8)$	$O(n^6)$	$O(m)$

and Tamaki [18] combined the kernelization result in [17] and an enumeration technique to device a fixed-parameter tractable (FPT) algorithm with running time in $2^{O(\rho)} + n^{O(1)}$. Since the number of crossings may be quadratic in m , such an FPT result yields an algorithm whose running time is $2^{O(m^2)}$. On the other hand, a trivial $2^{n \log n} O(m^2)$ -time exact algorithm for TLCM can be obtained by iteratively considering each of the possible $n! \in \Theta(2^{n \log n})$ vertex orderings, and by verifying whether the considered ordering yields less than ρ crossings (which can be done in $O(m^2)$ time by considering each pair of edges). To the best of our knowledge, however, no faster exact algorithm is known for this problem that performs asymptotically better than the simple one mentioned above. Observe that for positive instances of TLCM, m is upper bounded by $\sqrt[3]{\frac{15625 \cdot \rho \cdot n^2}{4608}}$ [3].

TLKP has not been proved to be NP-complete, and no FPT algorithm parameterized by k is known for this problem. A trivial $2^{n \log n} O(m^2)$ -time exact algorithm for TLKP can be devised analogously to the one for TLCM. Observe that for positive instances of TLKP and for $k > 5$, m is upper bounded by $\frac{125}{96} \sqrt{k} \cdot n$ [3].

TLQP is NP-complete [2]. If we assume that its natural parameter is the maximum number of allowed mutually crossing edges, then no FPT algorithm exists for it parameterized by this parameter (unless P=NP). A trivial $2^{n \log n} O(m^3)$ -time exact algorithm for TLQP can be devised analogously to the one for TLCM, where we have to test for the existence of crossings among triples of edges instead of pairs. Observe that for positive instances of TLQP, m is upper bounded by $2n - 4$ [3].

TLS is NP-complete [26]. Dujmovic et al. gave an FPT algortihm for TLS with $2^{O(\sigma^3)} n$ running time [10]. A trivial $O(m^\sigma n)$ -time exact algorithm for TLS performs a guess of σ edges to be removed. This yields $\binom{m}{\sigma} \in O(m^\sigma)$ possible choices. For each of them, a linear-time algorithm to test if the input is a forest of caterpillars (and, thus, it admits a 2-level planar drawing [11]) is invoked. Since caterpillars have at most $n - 1$ edges, we have that for positive instances of TLS, m is upper bounded by $n - 1 + \sigma$.

OPCM is NP-complete [19]. However, the optimum value of crossings can be approximated with an approximation ratio of $O(\log^2 n)$ [24]. Bannister and Eppstein [4] showed that OPCM is fixed-parameter tractable parameterized by ρ . To this aim, they exploit Courcelle's Theorem [7, 8], which provides a super-exponential dependency of the running time in this parameter. A trivial $2^{n \log n} O(m^2)$ -time exact algorithm for OPCM can be devised analogous to the one for TLCM. For positive instances of OPCM, m is upper bounded by $\sqrt[3]{37 \cdot \rho \cdot n^2}$ [24].

BT is NP-complete, even when $\tau = 2$ [28], in which case it coincides with the problem of testing whether the input graph is sub-Hamiltonian. This negative result implies that the problem does not admit FPT algorithms parameterized by τ (unless P=NP). A trivial $2^{n \log n + m \log \tau} O(\tau n)$ -time exact algorithm for BT can be obtained by iteratively considering each of the possible choices of a permutation for the vertex order and of an assignment of the edges to the τ pages. This yields $n! \cdot \tau^m \in \Theta(2^{n \log n + m \log \tau})$ possible choices. For each of these choices, τ calls to a linear-time outer-planarity testing algorithm are performed, one for each of the graphs induced by the τ pages, to decide whether the considered choice defines a solution. Since outerplanar graphs have at most $2n - 3$ edges and by the definition of BT, we have that for positive instances of BT, m is upper bounded by $\tau(2n - 3)$.

BS is NP-complete [29] and no FPT algorithm parameterized by σ is known for it. A trivial $O(m^\sigma n)$ -

time exact algorithm for BS can be devised analogously to the one for TLS. By the density of outerplanar graphs and by the definition of BS, we have that for positive instances of BS, m is upper bounded by $2n - 3 + \sigma$.

2 Preliminaries

For basic concepts related to graphs and their drawings, we refer the reader, e.g., to [9, 25]. For the standard notation we adopt to represent quantum gates and circuits, and for basic concepts about quantum computation, we refer the reader, e.g., to [21, 23].

Notation. Let k be a positive integer. To ease the description, we will denote the value $\lceil \log_2 k \rceil$ simply as $\log k$, and the set $\{0, \dots, k-1\}$ as $[k]$. We refer to any of the permutations of the integers in $[k]$ as a k -permutation. A k -set is a set of size k .

We denote the set of binary values $\{0, 1\}$ by \mathbb{B} . Consider a binary string s of length $a \cdot b$, for some $a, b \in \mathbb{N}$, i.e., $s \in \mathbb{B}^{a \cdot b}$. We often regard s as a sequence of a binary integers, each represented with b bits (where the specific a and b will always be clarified in the considered context). For $i \in [a]$, the i -th number in s , which we denote by $s[i]$, is given by the substring of s formed by the bits $s[b \cdot i][b \cdot i + 1] \dots s[b \cdot i + b - 1]$. Moreover, for $j \in [b]$, we denote by $s[i][j]$ the j -th digit of $s[i]$, where $s[i][0]$ is the least significant bit of $s[i]$.

Graph drawing. A *drawing* of a graph maps each vertex to a point in the plane and each edge to a Jordan arc between its end-vertices. In this paper, we only consider graph drawings that are *simple*, i.e., every two edges cross at most once and no edge crosses itself. A graph is *planar* if it can be drawn in the plane such that no two edges cross, i.e., it admits a *planar drawing*. A graph is k -*planar* (with $k \geq 0$), if it can be drawn in the plane such that each edge is crossed at most k times, i.e., it admits a k -*planar drawing*. Finally, a graph is *quasi-planar*, if it can be drawn in the plane so that no three edges pairwise cross, i.e., it admits a *quasi-planar drawing*.

Let G be a graph. A τ -page book layout of G consists of a linear ordering \prec of the vertices of G along a line, called the *spine*, and of a partition $\{E_1, \dots, E_\tau\}$ of the edges of G into τ sets, called *pages*. A τ -page book embedding of G is a τ -page book layout such that no two edges of the same page cross. That is, there exist no two edges (u, v) and (w, z) in the same page E_i such that $u \prec v$, $v \prec w$, $u \prec z$, and $z \prec v$. The *book thickness* of G is the minimum integer τ for which G has a τ -page book embedding. The *book skewness* of G is the minimum number of edges that need to be removed from G so that the resulting graph has book thickness 1, that is, it is outerplanar [5].

Let $G = (U, V, E)$ be a bipartite graph, where U and V denote the two subsets of the vertex set of G , and E denotes the edge set of G . A 2-level drawing of G maps each vertex $u \in U$ to a point on a horizontal line ℓ_u , which we call the *u-layer*, each vertex $v \in V$ to a point on a horizontal line ℓ_v (distinct from ℓ_u), which we call the *v-layer*, and each edge in E to a y -monotone curve between its endpoints. Observe that, from a combinatorial standpoint, a 2-level drawing Γ of G is completely specified by the linear ordering in which the vertices in U and the vertices in V appear along ℓ_u and ℓ_v , respectively. The 2-level skewness of G is the minimum number of edges that need to be removed from G so that the resulting graph admits a 2-level planar drawing, that is, it is a forest of caterpillars [11].

Next, we provide the definitions of the search problems we study concerning 2-level drawings of graphs.

TWO-LEVEL CROSSING MINIMIZATION (TLCM)

Input: A bipartite graph G and a positive integer ρ .
Output: A 2-level drawing of G with at most ρ crossings, if one exists.

TWO-LEVEL k -PLANARITY (TLKP)

Input: A bipartite graph G and a positive integer k .
Output: A 2-level k -planar drawing of G , if one exists.

TWO-LEVEL QUASI PLANARITY (TLQP)

Input: A bipartite graph G .
Output: A 2-level quasi-planar drawing of G , if one exists.

TWO-LEVEL SKEWNESS (TLS)

Input: A bipartite graph G and an integer σ .

Output: A set $S \subseteq E(G)$ such that $|S| \leq \sigma$ and the graph $G' = (V, E(G) \setminus S)$ is a forest of caterpillars, if one exists.

Finally, we provide the definitions of the search problems we study concerning book embeddings of graphs.

ONE-PAGE CROSSING MINIMIZATION (OPCM)

Input: A graph G and a positive integer ρ .

Output: A 1-page book layout of G with at most ρ crossings, if one exists.

BOOK THICKNESS (BT)

Input: A graph G and an integer τ .

Output: A τ -page book embedding of G , if one exists.

BOOK SKEWNESS (BS)

Input: A graph G and an integer σ .

Output: A set $S \subseteq E(G)$ such that $|S| \leq \sigma$ and the graph $G' = (V, E(G) \setminus S)$ is outerplanar, if one exists.

Cross-independent sets. Let X be a ground set. Let X_k be the set of all k -sets of distinct elements of X , i.e., $X_k = \{\{a_1, a_2, \dots, a_k\} \mid \forall i \neq j : a_i \neq a_j; a_i, a_j \in X\}$. A subset S of X_k is *cross-independent* if, for any two k -sets $s_i, s_j \in S$, it holds that $s_i \cap s_j = \emptyset$. In order to prove the depth bounds of our circuits we will exploit the following.

Lemma 2.1. *The set X_k of all k -sets of distinct elements of a set X can be partitioned in $O(\sqrt{k^k} \cdot |X|^{k-1})$ cross-independent sets of size at most $\lfloor \frac{|X|}{k} \rfloor$, if $k < \frac{|X|+2}{3}$.*

Proof. The fact that a cross-independent subset S of X_k contains at most $\lfloor \frac{|X|}{k} \rfloor$ elements is trivial, since each element of S is a k -set and no two elements of S may contain the same element of X . To show that X_k admits a partition into $O(\sqrt{k^k} \cdot |X|^{k-1})$ cross-independent sets we proceed as follows. Consider the auxiliary graph $\mathcal{A}(X_k)$, whose vertices are in 1-to-1 correspondence with the elements of X_k , i.e., the k -sets of distinct elements of X . The edges of $\mathcal{A}(X_k)$ connect pairs of vertices corresponding to k -sets with a non-empty intersection. We show that the maximum degree of $\mathcal{A}(X_k)$ is $O(\sqrt{k^k} \cdot |X|^{k-1})$. This immediately implies that $\mathcal{A}(X_k)$ admits a proper coloring with $O(\sqrt{k^k} \cdot |X|^{k-1})$ colors. Since each color class induced an independent set in $\mathcal{A}(X_k)$, we have that the vertices of $\mathcal{A}(X_k)$ in the same color class form a cross-independent set, which yields the proof that $O(\sqrt{k^k} \cdot |X|^{k-1})$ cross-independent sets suffice to partition X_k .

We denote each vertex v of $\mathcal{A}(X_k)$ by the corresponding k -set $\{a_1, a_2, \dots, a_k\}$ in X_k . Recall that v is adjacent to all the vertices of $\mathcal{A}(X_k)$ whose corresponding sets contain at least one of a_1, a_2, \dots, a_k . We have that the number of vertices of $\mathcal{A}(X_k)$ that contain a subset of $\{a_1, a_2, \dots, a_k\}$ of size r is $\binom{k}{r} \binom{|X|-k}{k-r}$. Therefore, the degree of v is upper bounded by

$$\sum_{i=1}^{k-1} \binom{k}{i} \binom{|X|-k}{k-i} \quad (1)$$

Note that, the term $t_1(i) = \binom{k}{i}$ is maximum when $i = \frac{k}{2}$, i.e., when $t_1(\frac{k}{2}) = \binom{k}{\frac{k}{2}} \in O(\sqrt{k^k})$. On the other hand, the term $t_2(i) = \binom{|X|-k}{k-i} \in O(|X|^{k-i})$ is monotone as long as $k-i < \frac{|X|-k}{2}$, i.e., $k < \frac{|X|+2i}{3}$. Therefore, since $1 \leq i \leq k-1$, we get that $t_2(i)$ is monotone under our hypothesis that $k < \frac{|X|+2}{3}$. Therefore, if $k < \frac{|X|+2}{3}$, we get that Eq. (1), which can we rewritten as $\sum_{i=1}^{k-1} t_1(i)t_2(i)$, is upper bounded by $t_1(\frac{k}{2}) \sum_{i=1}^{k-1} |X|^{k-i} \leq \binom{k}{\frac{k}{2}} \cdot 2|X|^{k-1}$. This shows the claimed bound. \square

We remark that, for $k = 2$, the asymptotic bounds of Lemma 2.1 can also be derived from Vizing's Theorem [27].

Mathematical formulations. We introduce the mathematical formulations used in the the D-Wave quantum annealing platform.

A *constrained binary optimization* (CBO) is the mathematical formulation of an optimization problem, in which the variables are binary. Note that, both the objective function and the constraints may have an arbitrary degree. In some cases, we focus on CBO formulations in which the objective function is not defined, and we aim at verifying whether a problem instance satisfies the given constraints.

A *quadratic unconstrained binary optimization* (QUBO) is the mathematical formulation of an optimization problem, in which the variables are binary, the optimization function is quadratic, and there are no constraints. Specifically, let Q be an upper triangular matrix $Q \in \mathbb{R}^{k \times k}$. Using Q , we can define a quadratic function $f_Q : \mathbb{B}^k \rightarrow \mathbb{R}$ that assigns a real value to a k -length binary vector. Namely, we let $f_Q(x) = x^T Q x = \sum_{i=1}^k \sum_{j=1}^k Q_{ij} x_i x_j$. The QUBO formulation for f_Q asks for the binary vector x^* that minimizes f_Q , i.e., $x^* = \arg \min_{x \in \mathbb{B}^k} f_Q(x)$.

3 Basic Quantum Circuits

In this section, we introduce basic quantum circuit which we will exploit in Sects. 5 and 6. Let D be a vertex-weighted directed acyclic graph (DAG). The *depth* of D is the number of vertices in a longest path of D . Two vertices u and v of D are *incomparable* if there exists no directed path from u to v , or vice versa. An *anti-chain* of D is a maximal set of incomparable vertices. The *weight* of an anti-chain is the sum of its vertex weights. The *width* of D is the maximum weight of an anti-chain of D . A quantum circuit Q can be modeled as a vertex-weighted directed acyclic graph D_Q , whose vertices correspond to the gates of Q and whose directed edges represent qubit input-output dependencies. Moreover, the weight of a vertex representing a gate U corresponds to the number of elementary gates [21, 23] needed to build U .

The *circuit complexity* of a quantum circuit is the number of elementary gates used to construct it. The *depth* and the *width* of a quantum circuit are the depth and the width, respectively, of its associated weighted DAG. Note that, the size of a circuit corresponds to the total number of operations that must be performed to execute the circuit, the depth of a circuit corresponds to the number of distinct time steps at which gates are applied, and the width of a circuit corresponds to the maximum number of operations that can be performed “in parallel”. Therefore, it is natural to upper bound the time complexity either by its depth, assuming the gates at each layer can be executed in parallel, or by its circuit complexity, assuming the gates are executed sequentially. In the lemmas and theorems that will follow, we describe circuits in terms of their circuit complexity, depth, and width. The width of the circuit is reported as an indication of the desired level of parallelism.

We denote by $|0_k\rangle$ the quantum basis state composed of k qubits set to $|0\rangle$. We now describe some gates that will be used in the following sections. Let $\phi[i]$ and $\phi[j]$ be binary strings of length $\log t$, which we interpret as binary integers represented with $\log t$ bits. Also, let $|\phi[i]\rangle$ and $|\phi[j]\rangle$ be the basis states corresponding to $\phi[i]$ and $\phi[j]$, respectively. First, we focus on gate U_+ that, given integers $\phi[i]$ and $\phi[j]$, verifies if $\phi[i]$ is equal to $\phi[j]$.

Lemma 3.1. *There exists a gate U_+ that, when provided with the input superposition $|\phi[i]\rangle |\phi[j]\rangle |0_{\log t}\rangle |0\rangle$, produces the output superposition $|\phi[i]\rangle |\phi[j]\rangle |0_{\log t}\rangle |\phi[i] = \phi[j]\rangle$. Gate U_+ has $O(\log t)$ circuit complexity, depth, and width.*

Proof. Gate U_+ consists of two gates μ_+ and μ_-^{-1} and in between such gates it executes a Toffoli gate; refer to Fig. 1. The input of μ_+ is the superposition $|\phi[i]\rangle |\phi[j]\rangle |0_{\log t}\rangle$. The output of μ_+ is the superposition

$$|\phi[i]\rangle |\phi[j]\rangle |\phi[i][0] = \phi[j][0]\rangle \dots |\phi[i][\log(t) - 1] = \phi[j][\log(t) - 1]\rangle.$$

Gate μ_+ , for each $a \in [\log t]$, computes qubit $|\phi[i][a] = \phi[j][a]\rangle$ with two Toffoli gates with three inputs and outputs. The input to both Toffoli gates are the two control qubits $|\phi[i][a]\rangle$, $|\phi[j][a]\rangle$, and a target qubit initialized to $|0\rangle$. The first Toffoli gate is activated when $\phi[i][a] = \phi[j][a] = 1$. The second Toffoli gate is activated when $\phi[i][a] = \phi[j][a] = 0$. The target qubit is set to $|0 \oplus (\phi[i][a] = \phi[j][a])\rangle$. Qubits $|\phi[i][0] = \phi[j][0]\rangle \dots |\phi[i][\log(t) - 1] = \phi[j][\log(t) - 1]\rangle$ form the input of a Toffoli gate with $\log t + 1$ inputs and outputs, which computes qubit $|\phi[i] = \phi[j]\rangle$. The control qubits are $|\phi[i][0] = \phi[j][0]\rangle \dots |\phi[i][\log(t) - 1] = \phi[j][\log(t) - 1]\rangle$. The target qubit is initialized to $|0\rangle$. The Toffoli gate is activated if $|\phi[i][a] = \phi[j][a]\rangle$ is equal to $|1\rangle$, for all $a \in [\log t]$. The target qubit is set to $|0 \oplus \bigwedge_{a \in [\log t]} (\phi[i][a] = \phi[j][a])\rangle$. The qubits

$$|\phi[i]\rangle |\phi[j]\rangle |\phi[i][0] = \phi[j][0]\rangle \dots |\phi[i][\log(t) - 1] = \phi[j][\log(t) - 1]\rangle$$

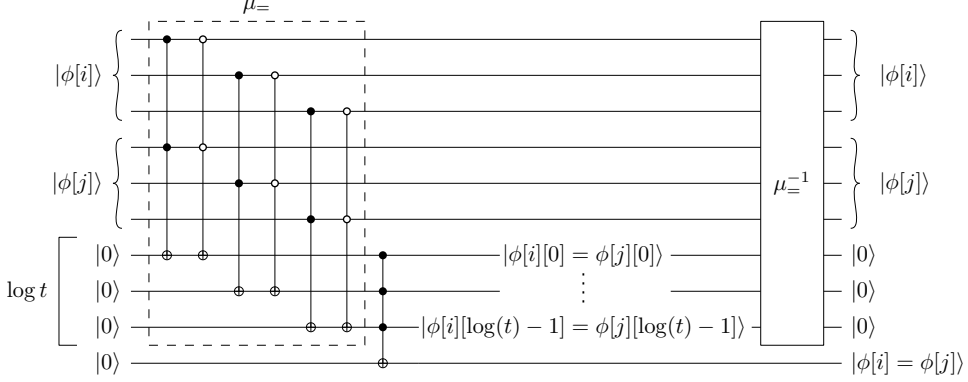


Figure 1: The gate $U_$.

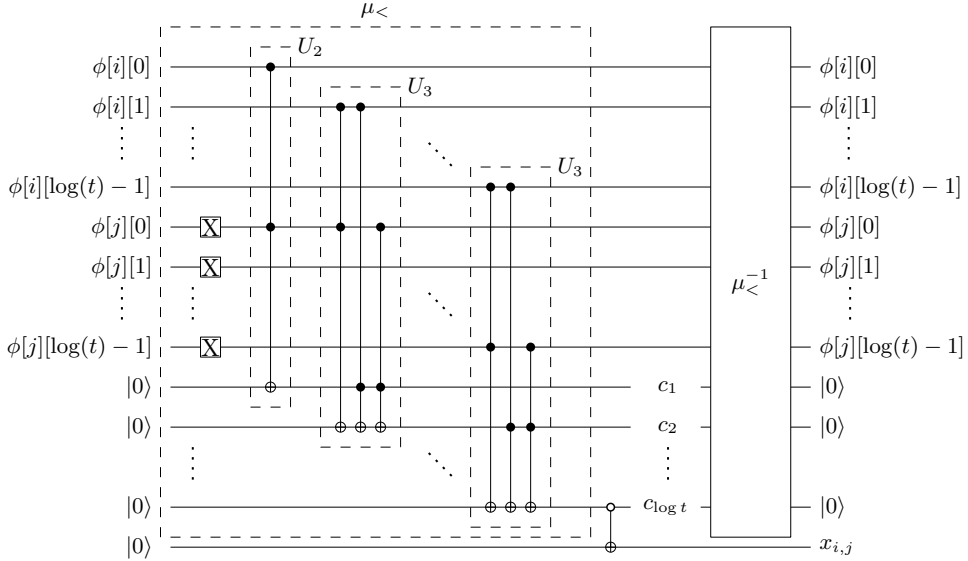


Figure 2: The gate $U_<$.

then enter $\mu_-=^{-1}$ that, being the inverse of μ_- , outputs the superposition $|\phi[i]\rangle|\phi[j]\rangle|0_{\log t}\rangle$. Overall, U_- is implemented using $4\log t$ Toffoli gates with a constant number of inputs and outputs and one Toffoli gate with $\log t + 1$ inputs and outputs. In turn, this last Toffoli gate is implemented using $\log t$ Toffoli gates with $O(1)$ inputs and outputs. Gate U_- has circuit complexity $O(\log t)$. Hence, it has the same bound for its depth and width. \square

Second, we focus on gate $U_<$ that, given binary integers $\phi[i]$ and $\phi[j]$ represented with $\log t$ bits, verifies if $\phi[i]$ is less than $\phi[j]$.

Lemma 3.2. *There exists a gate $U_<$ that, when provided with the input superposition $|\phi[i]\rangle|\phi[j]\rangle|0_{\log t}\rangle|0\rangle$, produces the output superposition $|\phi[i]\rangle|\phi[j]\rangle|0_{\log t}\rangle|\phi[i] < \phi[j]\rangle$. Gate $U_<$ has $O(\log t)$ circuit complexity, depth, and width.*

Proof. Gate $U_<$ consists of two gates $\mu_<$ and $\mu_<^{-1}$ and in between such gates it executes an Anticontrolled NOT gate; refer to Fig. 2. The input of $\mu_<$ is the superposition $|\phi[i]\rangle|\phi[j]\rangle|0_{\log t}\rangle|0\rangle$. The output of $\mu_<$ is the superposition $|\phi[i]\rangle|\phi[j]\rangle|c_0\rangle|c_2\rangle\dots|c_{\log(t)-1}\rangle$, where c_0 is the carry of the sum $\phi[i][0] + \phi[j][0]$ and c_k is equal to the carry of the sum of $c_{k-1} + \phi[i][k] + \phi[j][k]$, with $2 \leq k < \log n$.

Gate $\mu_<$ uses two gates U_2 and U_3 . Gate U_2 computes the carry of the sum of two qubits, receiving as input $|a\rangle|b\rangle|0\rangle$ and outputs $|a\rangle|b\rangle|a \wedge b\rangle$. Gate U_3 computes the carry of the sum of three qubits, receiving as input $|a\rangle|b\rangle|c\rangle|0\rangle$ and outputs $|a\rangle|b\rangle|c\rangle|(a \wedge b) \vee (a \wedge c) \vee (b \wedge c)\rangle$. Gate $\mu_<$ first computes the complement to one $\phi[j]$ of $\phi[j]$, using bit-flip (Pauli-X) gates, then it performs U_2 between $\phi[i][0]$ and $\overline{\phi[j][0]}$. The carry qubit of the previous sum, together with $\phi[i][1]$ and $\overline{\phi[j][1]}$ enters U_3 . For $k = 2, \dots, \log(t) - 1$ it performs the U_3 gate between the carry qubit of the previous sum, and $\phi[i][k]$ and $\overline{\phi[j][k]}$. Note that, the last carry qubit is equal to one if and only if $\phi[i]$ is greater than $\phi[j]$.

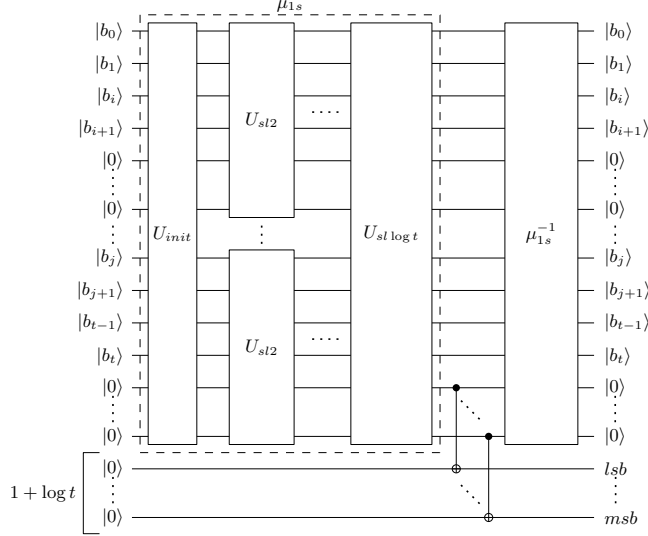


Figure 3: Structure of gate U_{1s} .

The last carry qubit of $\mu_<$ is used as the input control qubit of a ANTICONTROLLED NOT gate whose input target qubit is set to $|0\rangle$. The output target qubit is therefore “flipped” only if the input control qubit is $|0\rangle$, i.e., if $\phi[i] < \phi[j]$.

All qubits, except for the one computed above, now enter gate $\mu_<^{-1}$ that is the inverse gate of $\mu_<$.

Overall, $U_<$ is implemented using $2 \log t$ Pauli-X gates with one input and one output, and $6 \log t + 2$ Toffoli gates with three inputs and outputs. Plus, it uses an Anticontrolled NOT, with two inputs and outputs. This shows that the circuit complexity of $U_<$ is $O(\log t)$. Hence, it has the same bound for the depth and for the width. \square

Third, we focus on gate U_{1s} that, given a binary string b of length t , counts how many bits set to 1 are in it. For simplicity, we assume that t is a power of 2. If not, we can always append to b the smallest number of 0s such that this property holds. Observe that, in the worst case, the length of the string may double, which does not alter the asymptotic bounds of the next lemma.

Lemma 3.3. *There exists a gate U_{1s} that, when provided with the input superposition $|b_0 \dots b_{t-1}\rangle |0_h\rangle |0_k\rangle$, where t is a power of 2, $k = 1 + \log t$, and $h = 4t - 2\log t - 4$, produces the output superposition $|b_0 \dots b_{t-1}\rangle |0_h\rangle |s\rangle$, where s is the binary representation, in $\log t + 1$ bits, of the total number $\sum_{i=0}^{t-1} b_i$ of qubits set to 1 in b . Gate U_{1s} has $O(t)$ circuit complexity, $O(\log^2 t)$ depth, and $O(t)$ width.*

Proof. Gate U_{1s} consists of two gates μ_{1s} and μ_{1s}^{-1} , and in between such gates it executes $\log(t) + 1$ C-NOT gates; refer to Fig. 3. Let $b = b_0 \dots b_{t-1}$, i.e., b_i is the i -th bit of the binary string b . The input of μ_{1s} is the superposition $|b\rangle |0_{h-1-\log t}\rangle |0_{1+\log t}\rangle$. Gate μ_{1s} outputs the superposition $|b\rangle |0_{h-1-\log t}\rangle |s\rangle$, where $s = \sum_{i=0}^{t-1} b_i$ is the binary representation, in $\log t + 1$ qubits, of the total number of bits set to 1 in b .

Gate μ_{1s} exploits the gate U_{init} and the gates $U_{sl(i)}$, for $i = 2, \dots, \log(t)$; refer to Fig. 4. Specifically, μ_{1s} first executes the gate U_{init} . Then, it executes $\frac{t}{4}$ parallel gates $U_{sl(2)}$. Then, for $i = 3, \dots, \log(t)$, in gate μ_{1s} , the $\frac{t}{2^{i-1}}$ parallel gates $U_{sl(i-1)}$ are followed by $\frac{t}{2^i}$ parallel gates $U_{sl(i)}$; refer to Fig. 4.

The purpose of gate U_{init} is to “transform” the binary string b of length t in $\frac{t}{2}$ binary strings bn_i each of length 2, such that bn_i is the binary encoding of the number $b_{2i} + b_{2i+1}$, for $i = 0, \dots, \frac{t-2}{2}$. Namely, this gate partitions the bits of b into pairs and sums each pair to form a binary integer represented using two bits. Gate U_{init} exploits $\frac{t}{2}$ parallel gates HALF-ADDER (HA) U_h , which we describe next; refer to Fig. 5a. Each gate HA takes in input the superposition $|ab\rangle |0\rangle |0\rangle$, where $a, b \in \mathbb{B}$, and outputs the superposition $|ab\rangle |z\rangle |c\rangle$, where $z = a \oplus b$ is the least significant bit of the binary sum $a + b$ and $c = a \wedge b$ is the most significant bit of the binary sum $a + b$. Observe that, c is the carry bit of the bitwise sum of a and b . For each $i = 0, \dots, \frac{t-2}{2}$, the U_{init} exploits a gate HA to which the bits b_{2i} and b_{2i+1} are provided in place of the bits a and b , respectively; see Fig. 4. Note that, each gate HA has $O(1)$ circuit complexity, depth, and width. Thus, the gate U_{init} has $O(t)$ circuit complexity, $O(1)$ depth, and $O(t)$ width.

The purpose of the gate $U_{sl(i)}$ is to compute the sum of two binary integers of length i , which it then outputs as a binary integer of length $i + 1$. This gate exploit 1 gate HA and $i - 1$ gates FULL-ADDER (FA)

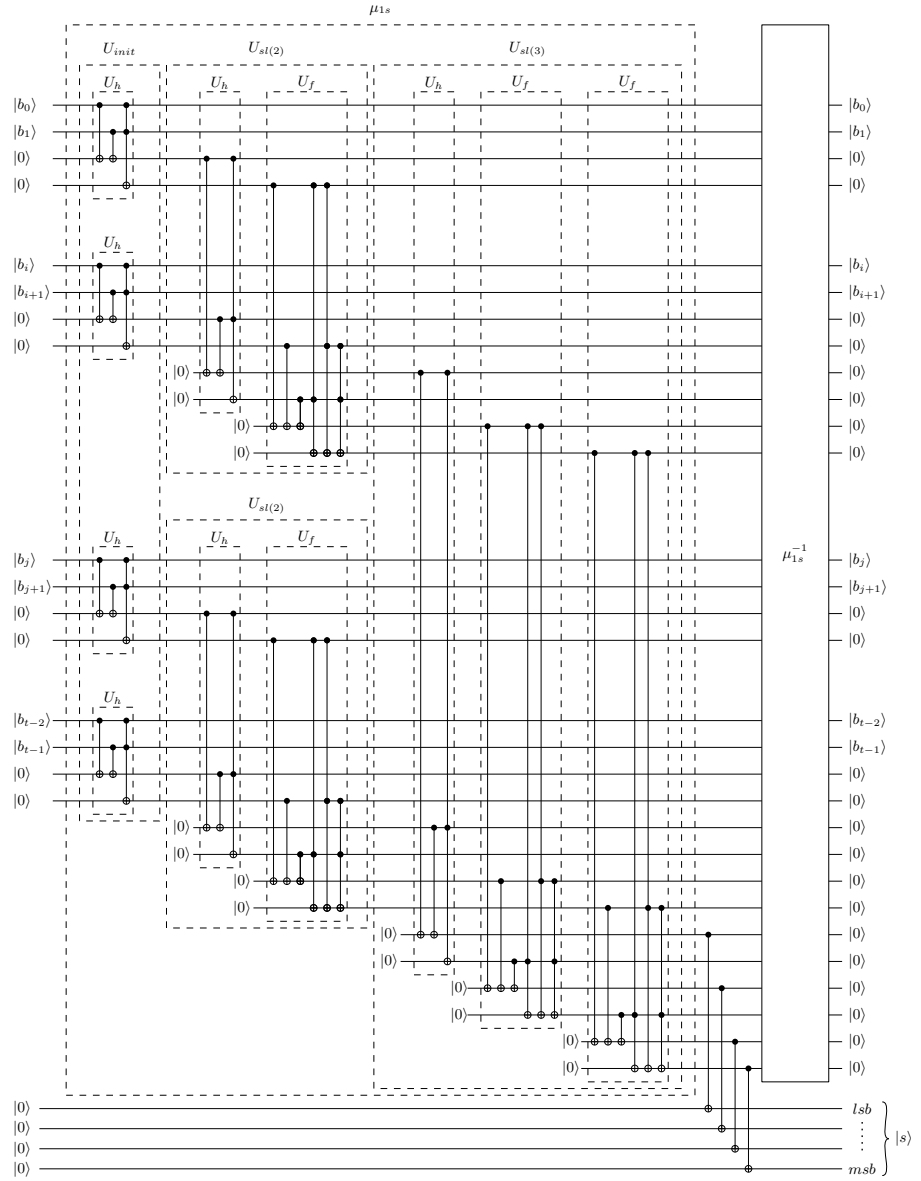


Figure 4: First three steps of gate U_{1s} , with $t = 8$.

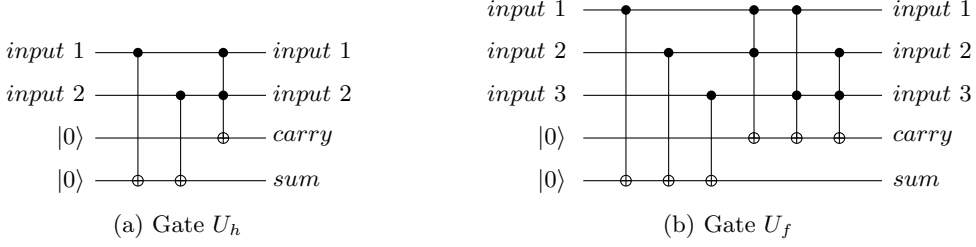


Figure 5: The half-adder gate U_h (left) and the full-adder gate U_f (right).

U_f , which we describe next; refer to Fig. 5b. Each gate FA takes in input the superposition $|abc\rangle|0\rangle|0\rangle$, where $a, b, c \in \mathbb{B}$, and outputs the superposition $|abc\rangle|z\rangle|c\rangle$, where $z = a \oplus b \oplus c$ is the least significant bit of the binary sum $a + b + c$ and $c = (a \wedge b) \vee (a \wedge c) \vee (b \wedge c)$ is the most significant bit of the binary sum $a + b + c$. Observe that, c is the carry bit of the bitwise sum of a , b , and c . The gate $U_{sl(i)}$ uses a gate HA to compute the sum of the two least significant bits of its two input binary integers; let c_0 be the corresponding carry bit (possibly $c_0 = 0$). Then, it uses a gate FA to compute the sum of the carry bit c_0 with the second-least significant bit of the two input binary integers; let c_1 be the corresponding carry bit. Then, for $k = 1, \dots, i-1$, it uses a gate FA to compute the sum of the carry bit c_k with the $(k+1)$ -th least-significant bit of the two input binary integers. Note that, each gate FA has $O(1)$ circuit complexity, depth, and width. Thus, the gate $U_{sl(i)}$ has $O(i)$ circuit complexity, $O(i)$ depth, and $O(1)$ width. Altogether, the gate $U_{sl(i)}$ takes in input the superposition $|a_0 \dots a_{i-1}\rangle|b_0 \dots b_{i-1}\rangle|0_{2i}\rangle$, where $a_0, \dots, a_{i-1}, b_0, \dots, b_{i-1} \in \mathbb{B}$, and outputs the superposition $|a_0 \dots a_{i-1}\rangle|b_0 \dots b_{i-1}\rangle|z\rangle|c\rangle|g\rangle$, where $z \in \mathbb{B}^i$, $c = c_i \in \mathbb{B}$, and the binary string cz coincides with $a_0a_1 \dots a_{i-1} + b_0b_1 \dots b_{i-1}$ and $g = c_0c_1 \dots c_{i-1}$ is the concatenation of the carry bits of the gate HA and of the gates FA. Since the gate $U_{sl(i)}$ consists of one gate HA and $i-1$ gates FA, it has $O(i)$ circuit complexity, $O(i)$ depth, and $O(1)$ width.

To prove some of the next bounds, we will exploit the following.

Claim 1. For any positive integer $k \geq 1$, let $\phi(k) = \sum_{i=1}^k \frac{i}{2^i}$. It holds that

$$\phi(k) = \frac{1}{2^k} (2^{k+1} - k - 2) \quad (2)$$

Proof. We prove the statement by induction on k .

In the base case $k = 1$. Then, by definition, $\phi(1) = \sum_{i=1}^1 \frac{i}{2^i} = \frac{1}{2}$. Also, by Eq. (2), $\phi(1) = \frac{1}{2}(4 - 1 - 2) = \frac{1}{2}$. Therefore, the statement holds.

Suppose now that $k > 1$. Then, by definition, we have

$$\phi(k) = \sum_{i=1}^k \frac{i}{2^i} = \sum_{i=1}^{k-1} \frac{i}{2^i} + \frac{k}{2^k} = \phi(k-1) + \frac{k}{2^k}. \quad (3)$$

By induction and by Eq. (2), we have that $\phi(k-1) = \frac{1}{2^{k-1}}(2^k - k - 1)$. Thus, by replacing $\phi(k-1)$ with such an expression in Eq. (3), we have

$$\begin{aligned} \phi(k) &= \frac{1}{2^{k-1}}(2^k - k - 1) + \frac{k}{2^k} = \\ &= \frac{1}{2^k}(2(2^k - k - 1) + k) = \frac{1}{2^k}(2^{k+1} - 2k - 2 + k) = \frac{1}{2^k}(2^{k+1} - k - 2). \end{aligned} \quad (4)$$

Eq. (4) concludes the proof of the inductive case and of the claim. \square

Since gate μ_{1s} contains a gate U_{init} and the gates $U_{sl(i)}$, for $i = 2, \dots, \log(t)$, we have the following. The circuit complexity of μ_{1s} can be estimated as follows. Gate U_{init} contains $\frac{t}{2}$ gates HA. Also, for $i = 2, \dots, \log(t)$, gate μ_{1s} contains $\frac{t}{2^i}$ gates $U_{sl(i)}$. Moreover, each gate $U_{sl(i)}$ contains a total number of gate HA and FA equal to i . Therefore, the overall number of gates HA and FA in μ_{1s} is $Y = t \cdot \sum_{i=1}^{\log t} \frac{i}{2^i}$. Since $Y = t \cdot \phi(\log t)$, by Claim 1 we have that $Y = 2t - \log(t) - 2$, which is in $O(t)$. Therefore, the circuit complexity of μ_{1s} is upper bounded by $O(t)$. The depth of μ_{1s} in $O(\sum_{i=1}^{\log t} i) \in O(\log^2 t)$. Finally, the width of μ_{1s} is bounded by the number of parallel circuits in U_{init} , which is $O(t)$.

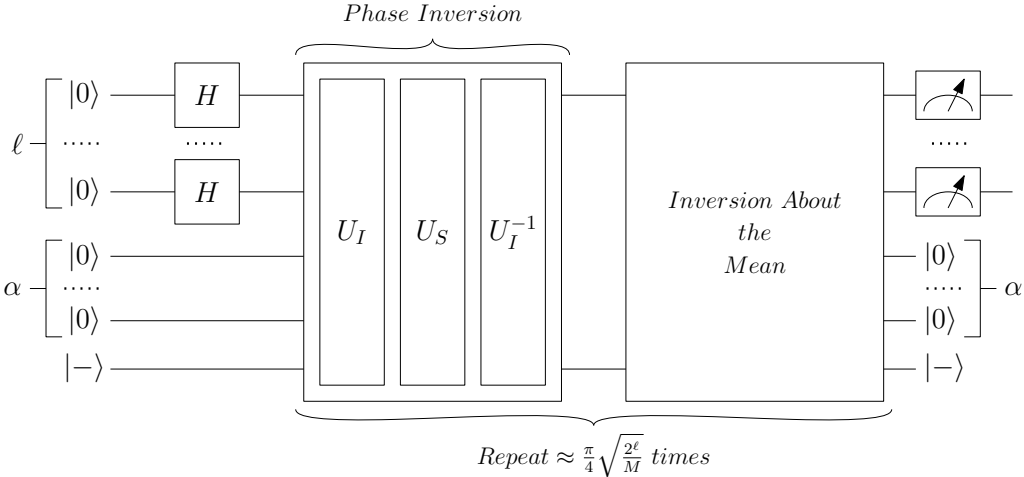


Figure 6: Overview of the quantum graph drawing framework based on Grover's approach.

Observe that, the circuit $U_{sl(\log t)}$ is the last circuit of μ_{1s} , and its output (which coincides with the one of μ_{1s}) is the superposition $|b\rangle|0_{h-1-\log t}\rangle|s\rangle$, where $s = \sum_{i=1}^t b_i$ is the binary representation, in $\log t + 1$ qubits, of the total number of bits set to 1 in b . In order to allow the reuse of the ancilla qubit of μ_{1s} , and still include the $\log t + 1$ qubits of s in the output of U_{1s} , the gate U_{1s} contains $\log t + 1$ C-NOT gates, which are then followed by the inverse circuit μ_{1s}^{-1} . In particular, the control qubit of each of these C-NOT gates is one of the $\log t + 1$ bits of s and the target qubit is initialized to $|0\rangle$. Since C-NOT gates have $O(1)$ circuit complexity, we have that the circuit complexity, depth, and width of the gate U_{1s} have the same asymptotic bounds of the circuit complexity, depth, and width of the gate μ_{1s} .

To complete the proof, we show the bounds on the number of ancilla qubit of the gate U_{1s} . First, observe that each C-NOT gate uses exactly one ancilla qubit, which it turned into one of the bits encoding the sum $\sum_{i=1}^t b_i$. Since $1 + \log t$ bits may be needed to encode such a sum, we use $1 + \log t$ C-NOT gates. This shows that $k = 1 + \log t$. For the value h , observe that each gate HA and FA used in the gates μ_{1s} and μ_{1s}^{-1} exploits two ancilla qubits. Therefore, the number h of ancilla qubits in input to μ_{1s} (and to μ_{1s}^{-1}) is $2Y = 2(2t - \log(t) - 2) = 4t - 2\log(t) - 4$. This concludes the proof. \square

4 A Quantum Framework for Graph Drawing Problems

In this section, we establish a framework for dealing with several NP-complete graph drawing problems; refer to Fig. 6. The framework is based on the Grover's approach for quantum search [14], which builds upon three circuits. The first circuit is a Hadamard gate that builds a uniform superposition of a sequence of qubits representing a potential, possibly not well-formed, solution to the problem. The second circuit exploits an *oracle* to perform the so-called PHASE INVERSION. The third circuit executes the so-called INVERSION ABOUT THE MEAN. The second and the third circuit are executed a number of times which guarantees that a final measure outputs a solution, if any, with high probability.

Theorem 4.1 (Grover's search [1, 14]). *Let P be a search problem whose solutions can be represented using ℓ bits and suppose that there exists a PHASE INVERSION circuit for P with $c(\ell)$ circuit complexity and $d(\ell)$ depth. Assume that $c(\ell)$ and $d(\ell)$ are $\Omega(\log \ell)$. Then, there exists a quantum circuit that outputs a solution for P , if any, with $\frac{\pi}{4}\sqrt{\frac{2^{\ell}}{M}} \cdot O(c(\ell))$ circuit complexity and $\frac{\pi}{4}\sqrt{\frac{2^{\ell}}{M}} \cdot O(d(\ell))$ depth, where M is the number of solutions of P .*

Let n and m be the number of vertices and edges of an input graph G , respectively. Observe that, in all the problems we consider, G admits the sought layout if and only if each of its connected components does. Hence, in the following, we assume that G is connected, and therefore $m \geq n - 1$. During the computation, we will manage a superposition $|\Gamma\rangle = |\Phi\rangle|\Psi\rangle|\Theta\rangle$, where $|\Phi\rangle$ is a superposition of $n \log n$ qubits, $|\Psi\rangle$ is a superposition of $m \log \tau$ qubits, and $|\Theta\rangle$ is a superposition of $\sigma \log m$ qubits. In particular, for some of the problems, $|\Psi\rangle$ and/or $|\Theta\rangle$ might not be present. We denote by ℓ the value $(n \log n) + (m \log \tau) + (\sigma \log m)$, where the second and/or third terms might be missing.

The superposition $|\Phi\rangle = \sum_{\phi \in \mathbb{B}^{n \log n}} c_{\phi} |\phi\rangle$ represents the superposition of all sequences of n natural numbers with values in $[n]$, each represented by a binary string ϕ of length $n \log n$ (according to notation

defined in Sect. 2 to represent sequences of integers). The digits corresponding to each natural number contained in ϕ form a consecutive sequence of length $\log n$. In particular, we denote by $\phi[i]$ the i -th natural number contained in ϕ . The purpose of $|\phi\rangle$ is to represent the position of each vertex of G in a total order. To this aim, observe that, within the superposition $|\Phi\rangle$, all possible states corresponding to assignments of positions from 0 to $n - 1$ for each vertex in G are included.

The superposition $|\Psi\rangle = \sum_{\psi \in \mathbb{B}^{m \log \tau}} c_\psi |\psi\rangle$ represents the superposition of all sequences of m natural numbers with values in $[\tau]$, each represented by a binary string ψ of length $m \log \tau$. The digits corresponding to each natural number contained in ψ form a consecutive sequence of length $\log \tau$. In particular, we denote by $\psi[i]$ the i -th natural number contained in ψ . The purpose of $|\psi\rangle$ is to represent a coloring of the edges of G with color in $[\tau]$. To this aim, observe that, within the superposition $|\Psi\rangle$, all possible states corresponding to an assignment of integers from 0 to $\tau - 1$ for each edge in G are included.

The superposition $|\Theta\rangle = \sum_{\theta \in \mathbb{B}^{\sigma \log m}} c_\theta |\theta\rangle$ represents the superposition of all sequences of σ natural numbers with values in $[m]$, each represented by a binary string θ of length $\sigma \log m$. The digits corresponding to each natural number contained in θ form a consecutive sequence of length $\log m$. In particular, we denote by $\theta[i]$ the i -th natural number contained in θ . The purpose of $|\theta\rangle$ is to represent a subset of the edges of G of size at most σ , each labeled with an integer in $[m]$. To this aim, observe that, within the superposition $|\Theta\rangle$, all possible states corresponding to a selection of σ edges of G , where each edge is indexed with an integer from 0 to $m - 1$, are included.

For problems TLCM, TLKP, TLQP, and OPCM, we have that $|\Gamma\rangle = |\Phi\rangle$. For problem BT, we have that $|\Gamma\rangle = |\Phi\rangle |\Psi\rangle$. Finally, for problems TLS and BS, we have that $|\Gamma\rangle = |\Phi\rangle |\Theta\rangle$.

Next, we present an overview of how the superposition $|\Gamma\rangle$ evolves within the three main circuits of the framework; refer to Fig. 6.

First, in all problems we study, ℓ qubits set to $|0\rangle$ enter an Hadamard gate that outputs the uniform superposition $|\Gamma\rangle = H^{\otimes \ell} |0_\ell\rangle = \frac{1}{\sqrt{2^\ell}} \sum_{\gamma \in \mathbb{B}^\ell} |\gamma\rangle$. Observe that, such a superposition, corresponds to the tensor product of the uniform superpositions $|\Phi\rangle = H^{\otimes n \log n} |0_{n \log n}\rangle$, $|\Psi\rangle = H^{\otimes m \log \tau} |0_{m \log \tau}\rangle$, and $|\Theta\rangle = H^{\otimes \sigma \log m} |0_{\sigma \log m}\rangle$, where possibly Ψ and/or Θ might be not present. Also, observe that, within $|\Gamma\rangle$, all possible solutions of the considered problems are included, if any exist.

Second, in Grover's approach, the INVERSION ABOUT THE MEAN circuit is prescribed. Hence, we now focus on the PHASE INVERSION circuit. In the first iteration, it receives as input (i) the uniform superposition $|\Gamma\rangle = H^{\otimes \ell} |0_\ell\rangle$, (ii) α ancilla qubits set to $|0\rangle$, whose number depends on the type of problem we are addressing, and (iii) a qubit set to $|-\rangle$. Namely, it receives as input the superposition $|\Gamma\rangle |0_\alpha\rangle |-\rangle$, where $|\Gamma\rangle = \frac{1}{\sqrt{2^\ell}} \sum_{\gamma \in \mathbb{B}^\ell} |\gamma\rangle$. It outputs the superposition $\frac{1}{\sqrt{2^\ell}} \sum_{\gamma \in \mathbb{B}^\ell} (-1)^{f(\gamma)} |\gamma\rangle |0_\alpha\rangle |-\rangle$, where $f(\gamma) = 1$ if and only if γ represents a valid solution to the considered problem. In general, the PHASE INVERSION circuit receives in input the superposition $|\Gamma\rangle |0_\alpha\rangle |-\rangle$, where $|\Gamma\rangle = \sum_{\gamma \in \mathbb{B}^\ell} c_\gamma |\gamma\rangle$. It outputs the the superposition $\sum_{\gamma \in \mathbb{B}^\ell} (-1)^{f(\gamma)} c_\gamma |\gamma\rangle |0_\alpha\rangle |-\rangle$. We remark that the values of the complex coefficients c_γ depend on the iteration.

For each problem we consider, we provide a specific PHASE INVERSION circuit. All such circuits consist of three circuits (see Fig. 6), the first is called INPUT TRANSDUCER and is denoted by U_I , the second is called SOLUTION DETECTOR and is denoted by U_S , and the third is the inverse U_I^{-1} of the INPUT TRANSDUCER. The purpose of the INPUT TRANSDUCER circuits is to “filter out” the states of $|\Gamma\rangle$ that do not correspond to “well-formed” candidate solutions. The purpose of the SOLUTION DETECTOR circuits is to invert the amplitude of the states of $|\Gamma\rangle$ that correspond to positive solutions, if any. The purpose of U_I^{-1} is to restore the state of the ancilla qubits to $|0\rangle$ so that they may be employed in the subsequent iterations of the amplitude-amplification process.

The INPUT TRANSDUCER circuits are described in Sect. 5. The SOLUTION DETECTOR circuits are described in Sect. 6. In that section, we also combine the INPUT TRANSDUCER circuits and the SOLUTION DETECTOR circuits to prove the following lemma; refer also to Table 1.

Lemma 4.2. *The TLCM, TLKP, TLQP, TLS, OPCM, BT, and BS problems admit PHASE INVERSION circuits whose circuit complexity, depth, and width are bounded as follows:*

TLCM *Circuit complexity: $O(m^2)$. Depth: $O(n^2)$. Width $O(m^2)$.*

TLKP *Circuit complexity: $O(m^2)$. Depth: $O(m \log^2 m)$. Width $O(m)$.*

TLQP *Circuit complexity: $O(m^6)$. Depth: $O(m^4)$. Width $O(m^2)$.*

TLS *Circuit complexity: $O(m^2)$. Depth: $O(m)$. Width $O(m)$.*

OPCM *Circuit complexity: $O(n^8)$. Depth: $O(n^6)$. Width $O(m^2)$.*

BT Circuit complexity: $O(n^8)$. Depth: $O(n^6)$. Width $O(m)$.

BS Circuit complexity: $O(n^8)$. Depth: $O(n^6)$. Width $O(m)$.

Theorem 4.1 and Lemma 4.2 imply the following.

Theorem 4.3. *In the quantum circuit model of computation, the TLCM, TLKP, TLQP, TLS, OPCM, BT, and BS problems can be solved with the following sequential and parallel time bounds (where M denotes the number of solutions to the problem):*

TLCM Sequential: $\sqrt{\frac{2^{n \log n}}{M}} \cdot O(m^2)$. Parallel: $\sqrt{\frac{2^{n \log n}}{M}} \cdot O(n^2)$.

TLKP Sequential: $\sqrt{\frac{2^{n \log n}}{M}} \cdot O(m^2)$. Parallel: $\sqrt{\frac{2^{n \log n}}{M}} \cdot O(m \log^2 m)$.

TLQP Sequential: $\sqrt{\frac{2^{n \log n}}{M}} \cdot O(m^6)$. Parallel: $\sqrt{\frac{2^{n \log n}}{M}} \cdot O(m^4)$.

TLS Sequential: $\sqrt{\frac{2^{n \log n + \sigma \log m}}{M}} \cdot O(m^2)$. Parallel: $\sqrt{\frac{2^{n \log n + \sigma \log m}}{M}} \cdot O(m)$.

OPCM Sequential: $\sqrt{\frac{2^{n \log n}}{M}} \cdot O(n^8)$. Parallel: $\sqrt{\frac{2^{n \log n}}{M}} \cdot O(n^6)$.

BT Sequential: $\sqrt{\frac{2^{n \log n + m \log \tau}}{M}} \cdot O(n^8)$. Parallel: $\sqrt{\frac{2^{n \log n + m \log \tau}}{M}} \cdot O(n^6)$.

BS Sequential: $\sqrt{\frac{2^{n \log n + \sigma \log m}}{M}} \cdot O(n^8)$. Parallel: $\sqrt{\frac{2^{n \log n + \sigma \log m}}{M}} \cdot O(n^6)$.

5 Input Transducer Circuits

We use two different versions of circuit U_I , depending on the considered problem. Namely, for all problems but for the TLS and the BS problems, circuit U_I consists of just one circuit U_{OT} , called ORDER-TRANSDUCER (refer to Fig. 7). For problems TLS and BS, circuit U_I executes, in parallel to U_{OT} , another circuit U_{ST} , called SKEWNESS-TRANSDUCER (refer to Fig. 10).

5.1 Order Transducer

Let ϕ be a binary string of length $n \log n$, which we interpret as a sequence of n binary integers, each consisting of $\log n$ bits. Recall that, we denote by $\phi[i]$ the i -th binary integer contained in ϕ . Also, let $|\phi\rangle$ be the basis state corresponding to ϕ . This subsection is devoted to proving the following lemma.

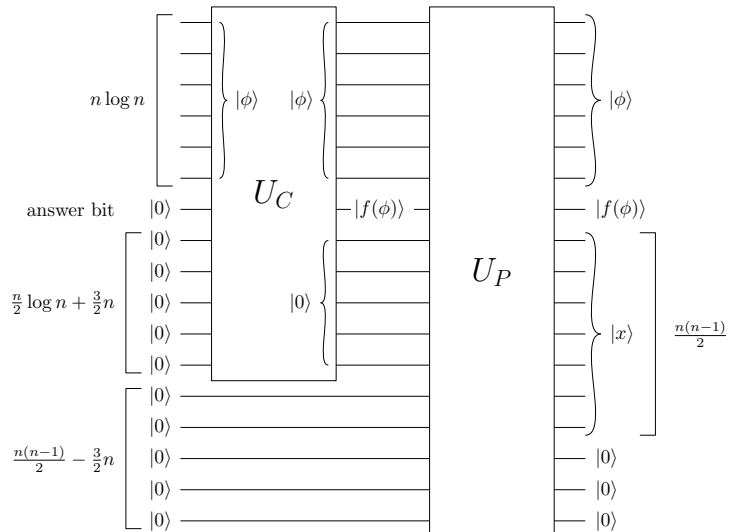


Figure 7: The ORDER TRANSDUCER gate U_{OT} .

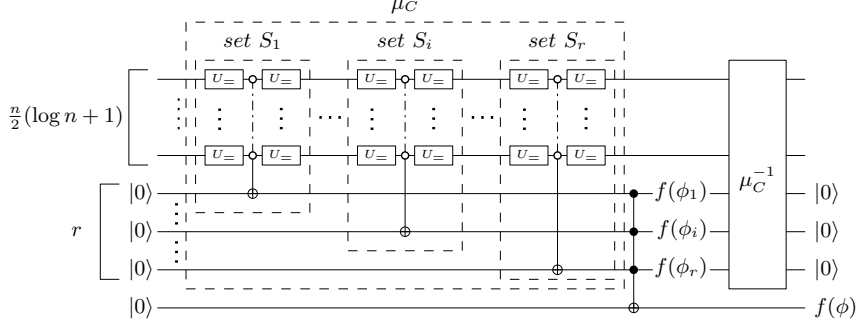


Figure 8: The gate U_C .

Lemma 5.1. *There exists a gate U_{OT} that, when provided with the input superposition $|\phi\rangle|0_\alpha\rangle$, where $\alpha = \frac{n}{2}(n-1 + \log n) + 1$, produces the output superposition*

$$|\phi\rangle|f(\phi)\rangle|x_{0,1}\rangle\dots|x_{0,n-1}\rangle\dots|x_{i,j}\rangle\dots|x_{n-2,n-1}\rangle|0_{\frac{n}{2}\log n}\rangle,$$

such that $|x_{i,j}\rangle = 1$ if and only if $\phi[i] < \phi[j]$ and $f(\phi) = 1$ if and only if ϕ represents an n -permutation. U_{OT} has $O(n^2 \log n)$ circuit complexity, and $O(n \log n)$ depth and width.

PROOF OF LEMMA 5.1. The input of U_{OT} is composed of $n \log n + \alpha$ qubits, the first $\ell = n \log n$ form a superposition $|\phi\rangle$ and the rest are set to $|0\rangle$. First, $|\phi\rangle$ and $\frac{n}{2}(\log n + 3) + 1$ qubits set to $|0\rangle$ enter a gate U_C , called COLLISION DETECTOR. The purpose of U_C is to compute the superposition $|\phi\rangle|f(\phi)\rangle|0_{\frac{n}{2}(\log n+3)}\rangle$, where $f(\phi) = 1$ if and only if $\phi[i] \neq \phi[j]$ for each $i \neq j$. It has $O(n^2 \log n)$ circuit complexity, and it has $O(n \log n)$ depth and width. Second, $|\phi\rangle$ and $\frac{n}{2} \log n + \frac{n(n-1)}{2}$ qubits set to $|0\rangle$ enter a gate U_P called PRECEDENCE CONSTRUCTOR. The purpose of U_P is to compute a superposition $|\phi\rangle|x\rangle|0_{\frac{n}{2}\log n}\rangle$, where $|x\rangle = |x_{0,1}\rangle\dots|x_{0,n-1}\rangle\dots|x_{i,j}\rangle\dots|x_{n-2,n-1}\rangle$ and $x_{i,j} = 1$ if and only if $\phi[i] < \phi[j]$. It has circuit complexity $O(n^2 \log n)$, and it has $O(n \log n)$ depth and width. Gate U_{OT} has $O(n^2 \log n)$ circuit complexity, and it has $O(n \log n)$ depth and width.

COLLISION-DETECTOR. Gate U_C works as follows. Refer to Fig. 8.

It executes two gates μ_C and μ_C^{-1} and in between such gates it executes a Toffoli gate. The input of μ_C is the superposition $|\phi[0]\rangle\dots|\phi[n-1]\rangle|0_{\frac{n}{2}(\log n+1)}\rangle|0_n\rangle$. The output of μ_C is the superposition $|\phi[0]\rangle\dots|\phi[n-1]\rangle|0_{\frac{n}{2}(\log n+1)}\rangle|f(\phi_0)\rangle\dots|f(\phi_i)\rangle\dots|f(\phi_{n-1})\rangle$. In gate μ_C , we compare the unordered pairs of numbers $\phi[i]$ and $\phi[j]$ in parallel as follows. Consider that if two numbers are compared, none of the two can be compared with another number at the same time. Hence, we partition the pairs using Lemma 2.1 (with $k = 2$ and $|X| = n$) into $r = O(n)$ cross-independent sets S_1, \dots, S_r each containing at most $\frac{n}{2}$ pairs.

For each pair (i, j) of S_1 (refer to Fig. 8) we use a $U_=_$ gate to compare $\phi[i]$ and $\phi[j]$. Recall that the gate $U_=_$ outputs a superposition $|\phi[i]\rangle|\phi[j]\rangle|0\rangle\dots|0\rangle|\phi[i] == \phi[j]\rangle$. All the last output qubits of the $U_=_$ gates for S_1 enter a Toffoli gate with $|S_1| + 1$ inputs and outputs, which computes the qubit $|f(\phi_0)\rangle$ such that $\phi_0 = 1$ if and only if all of them first $|S_1|$ input qubits are equal to $|0\rangle$, i.e., all pairs correspond to different numbers.

After dealing with S_1 , we deal with S_2 with the same technique and keep on dealing with the S_i sets until S_r is reached.

All the last output qubits of the $U_=_$ gates for S_i enter a Toffoli gate that outputs a qubit $|f(\phi_i)\rangle$ such that $f(\phi_i) = 1$ if and only if all of them are equal to $|0\rangle$, i.e., if does not exist pair (j, k) of S_i where $\phi[j] = \phi[k]$. In order to allow the reuse of the ancilla qubits, except for the qubit $|f(\phi_i)\rangle$, gate U_C executes in parallel a gate $U_=_^{-1}$ for each pair in S_i .

All the qubits $|f(\phi_i)\rangle$ and the qubit $|\phi\rangle$ enter a Toffoli gate with $r + 1$ inputs and outputs. The first r qubits are control qubits, the target qubit is $|f(\phi)\rangle$, which is initialized to $|0\rangle$. The target qubit is set to $|\bigwedge_{i=1}^r \phi_i\rangle$. In order to allow the reuse of the ancilla qubits, we apply to the entire circuit preceding the Toffoli gate its inverse gate. Recall that, by Lemma 3.1, gate $U_=_$ has $O(\log n)$ circuit complexity, depth, and width. Therefore, gate U_C has $O(n^2 \log n)$ circuit complexity, and it has $O(n \log n)$ depth and width.

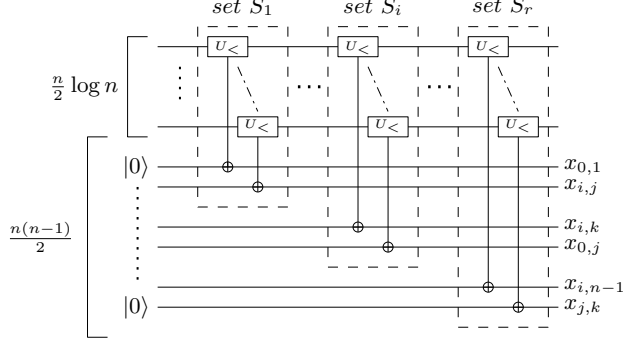


Figure 9: The gate U_P .

PRECEDENCE CONSTRUCTOR. Gate U_P works as follows. Refer to Fig. 9.

For each pair i, j ($i, j \in [n]$ and $i \neq j$) U_P exploits $U_<$ that outputs a qubit $|x_{i,j}\rangle$ such that $x_{i,j} = \phi[i] < \phi[j]$. Using several gates $U_<$, we compare the ordered pairs of numbers $\phi[i]$ and $\phi[j]$ in parallel as follows. As for gate U_C , if two numbers are compared, none of the two can be compared with another number at the same time. Hence, we partition the pairs using Lemma 2.1 (with $k = 2$ and $|X| = n$) into $r \in O(n)$ cross-independent sets S_1, \dots, S_r each containing at most $\frac{n}{2}$ pairs.

For each pair (i, j) of S_1 (refer to Fig. 9) we use a $U_<$ gate to compare $\phi[i]$ and $\phi[j]$. Recall that the gate $U_<$ outputs a superposition $|\phi[i]\rangle|\phi[j]\rangle|0\rangle\dots|0\rangle|\phi[i] < \phi[j]\rangle$. In order to allow the reuse of the ancilla qubit different from $|x_{i,j}\rangle$ for each pair $(i, j) \in S_1$, we use a symmetric circuit that transforms the ancilla output qubits into a sequence of $|0\rangle$ qubits, that will be re-used in the following step.

After dealing with S_1 , we deal with S_2 with the same technique and keep on dealing with the S_i sets until S_r is reached.

Recall that, by Lemma 3.2, gate $U_<$ has $O(\log n)$ circuit complexity, depth, and width. Therefore, gate U_P has $O(n^2 \log n)$ circuit complexity, and it has $O(n \log n)$ depth and width.

5.2 Skewness Transducer

Let θ be a binary string of length $\sigma \log m$, which we interpret as a sequence of σ binary integers, each consisting of $\log m$ bits. Recall that, we denote by $\theta[i]$ the i -th binary integer contained in θ . Also, let $|\theta\rangle$ be the basis state corresponding to θ . This subsection is devoted to proving the following lemma.

Lemma 5.2. *There exists a gate U_{ST} that, when provided with the input superposition $|\theta\rangle|0\rangle|0_m\rangle$, produces the output superposition $|\theta\rangle|f(\theta)\rangle|e_0\rangle\dots|e_i\rangle\dots|e_{m-1}\rangle$, such that $f(\theta) = 1$ if and only if θ represents a subset of size σ of the set $[m]$, and when $f(\theta) = 1$ it holds that $e_i = 1$ if and only if there exists $j \in [\sigma]$ such that $\theta[j]$ coincides with (the binary representation of) the integer i . Gate U_{ST} has $O(\sigma m \log m)$ circuit complexity and depth, and $O(\sigma \log m)$ width.*

PROOF OF LEMMA 5.2. The input of U_{ST} is composed of $\sigma \log m + 1 + m$ qubits, the first $\ell = \sigma \log m$ qubits form a superposition θ and the rest are set to $|0\rangle$. First, $|\theta\rangle, |0\rangle$, and $h = \frac{\sigma}{2}(\log m + 3)$ qubits set to $|0\rangle$ enter an instance of the COLLISION DETECTOR gate U_C used in the proof of Lemma 5.1, where the qubits of the superposition $|\theta\rangle|0\rangle|0_h\rangle$ play the role of the qubits of the superposition $|\phi\rangle|0\rangle|0_{\frac{n}{2}(\log n+3)}\rangle$. The purpose of this instance of U_C is to compute the superposition $|\theta\rangle|f(\theta)\rangle|0_h\rangle$, where $f(\theta) = 1$ if and only if $\theta[a] \neq \theta[b]$ for each $0 \leq a < b \leq \sigma - 1$. It has $O(\sigma^2 \log m)$ circuit complexity and it has $O(\sigma \log(m))$ depth and width. Second, the superpositions $|\theta\rangle$ and $|0_m\rangle$ enter a gate U_E , called EDGE CONSTRUCTOR; refer to Fig. 11a. The purpose of U_E is to compute the superposition $|\theta\rangle|e\rangle$, where $|e\rangle = |e_0\rangle\dots|e_i\rangle\dots|e_{m-1}\rangle$ and, when $f(\theta) = 1$, it holds that $e_i = 1$ if and only if there exists a $j \in [\sigma]$ such that $\theta[j]$ coincides with (the binary representation of) the integer i . It has $O(\sigma m \log m)$ circuit complexity, $O(\sigma m)$ depth, and $O(\log m)$ width. Recall that, $\sigma < m$. Thus, we have that gate U_{ST} has $O(\sigma m \log m)$ circuit complexity, $O(\sigma m)$ depth, and $O(\sigma \log m)$ width.

EDGE CONSTRUCTOR. The gate U_E exploits instances of the auxiliary gate U_{e_i} , defined for each edge $e_i \in E$ as follows. Refer to Fig. 11b. When provided with the input superposition $|\theta\rangle|0\rangle$, the gate

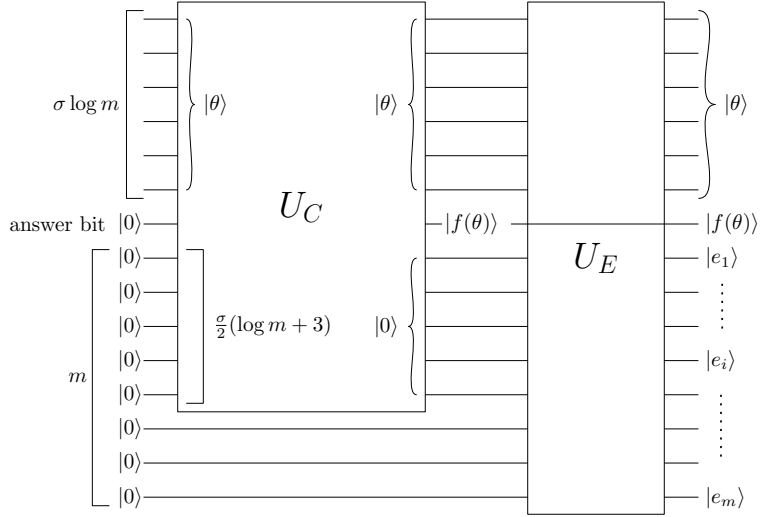


Figure 10: The SKEWNESS TRANSDUCER gate U_{ST} .

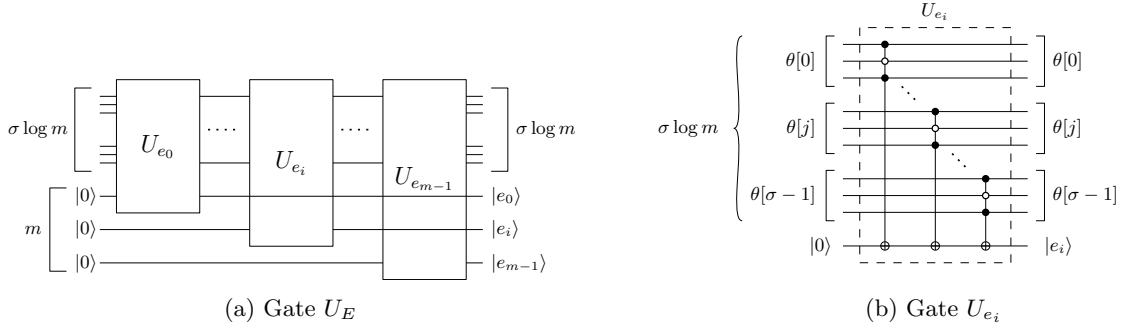


Figure 11: Illustration for the construction of gate U_E .

U_{e_i} produces the output superposition $|\theta\rangle|e_i\rangle$, where – provided that θ represents a subset of size σ of the set $[m]$, i.e., $f(\theta) = 1$ – it holds that $e_i = 1$ if and only if there exists $j \in [\sigma]$ such that $\theta[j]$ coincides with the integer i . The gate U_{e_i} contains σ Toffoli gates, each with $\log(m) + 1$ inputs and outputs. All such Toffoli gates share the same target qubit. The control qubits of the first Toffoli gate T_0 are $|\theta[0][0]\rangle \dots |\theta[0][\log(m)-1]\rangle$ and its target qubit is initialized to $|0\rangle$. It turns the target qubit into $|1\rangle$ if and only if $\theta[0][0] \dots \theta[0][\log(m)-1]$ coincides with the integer i . For $j = 1, \dots, \sigma - 1$, gate U_{e_i} contains a Toffoli gate T_j that takes in input the superposition $|\theta[j][0]\rangle \dots |\theta[j][\log(m)-1]\rangle$ and the target qubit that has been output by T_{j-1} . It flips the value of the target qubit if and only if $\theta[j][0] \dots \theta[j][\log(m)-1]$ coincides with (the binary representation of) the integer i . Thus, if at most one of the j integers composing θ coincides with the integer i , then $e_i = 1$ if and only if there exists $j \in [\sigma]$ such that $\theta[j]$ coincides with (the binary representation of) the integer i . Gate U_{e_i} has $O(\sigma \log m)$ circuit complexity, $O(\sigma)$ depth, and $O(\log m)$ width.

The gate U_E computes $|e\rangle = |e_0\rangle \dots |e_i\rangle \dots |e_{m-1}\rangle$ as follows. For $i \in [m]$, it computes $|e_i\rangle$ by applying the gate U_{e_i} to the superposition $|\theta\rangle|0\rangle$, where the last qubit is the i -th qubit of the m qubits compositing the superposition $|0_m\rangle$, which is provided in input to the gate U_E . Gate U_E has circuit complexity $O(\sigma m \log m)$, depth $O(\sigma m)$, and width $O(\log m)$.

6 Solution Detector Circuits

In this section, we present the details of the SOLUTION DETECTOR circuits U_S for the problems we consider.

Recall that, the ORDER TRASDUCER circuit produces the output superposition

$$|\phi\rangle|f(\phi)\rangle|x_{0,1}\rangle \dots |x_{0,n-1}\rangle \dots |x_{i,j}\rangle \dots |x_{n-2,n-1}\rangle|0_{\frac{n}{2}\log n}\rangle,$$

such that $x_{i,j} = 1$ if and only if $\phi[i] < \phi[j]$, and $f(\phi) = 1$ if and only if ϕ represents an n -permutation. In the following, for simplicity, we denote the superposition $|x_{0,1}\rangle \dots |x_{0,n-1}\rangle \dots |x_{i,j}\rangle \dots |x_{n-2,n-1}\rangle$ as $|x\rangle$. We interpret the values $x_{0,1}, \dots, x_{0,n-1}, \dots, x_{i,j}, \dots, x_{n-2,n-1}$ as the entries above the main diagonal of a square binary matrix X , where $X[i][j] = x_{i,j}$, and whose entries along and below the main diagonal are undefined. We use such entries to represent the precedence between vertices in a graph drawing. Let x be the string obtained by concatenating $x_{0,1}, \dots, x_{0,n-1}, \dots, x_{i,j}, \dots, x_{n-2,n-1}$. We will use x both for book layouts and for 2-level drawings as follows.

Consider book layouts of a graph $G = (V, E)$. We denote by $\Pi(x)$ the vertex order along the spine of a book layout of G defined as follows. We have that, if $x_{i,j} = 1$, then vertex v_i precedes vertex v_j in $\Pi(x)$. Conversely, if $x_{i,j} = 0$, then vertex v_j precedes vertex v_i in $\Pi(x)$. Consider now a 2-level drawing of a graph $G = (U, V, E)$. We assume that the vertices in U are labeled as $u_0, \dots, u_{|U|-1}$, and the vertices of V are labeled as $v_{|U|}, \dots, v_{|U|+|V|-1}$. We denote by $D(x)$ the 2-level drawing of G defined as follows. Let w_i and w_j be two vertices of G . Suppose that $w_i, w_j \in U$. If $x_{i,j} = 1$, then $w_i \prec w_j$ along the horizontal line ℓ_u , otherwise, $w_j \prec w_i$ along ℓ_u . Suppose that $w_i, w_j \in V$. If $x_{i,j} = 1$, then $w_i \prec w_j$ along the horizontal line ℓ_v , otherwise, $w_j \prec w_i$ along ℓ_v . Suppose now that $w_i \in U$ and $w_j \in V$. Then, we assume that $x_{i,j} = 0$, which we interpret as the absence of a precedence relation between such vertices.

We remark that, if ϕ is not an n -permutation, then $\Pi(x)$ and $D(x)$ do not correspond to actual spine orders and 2-level drawings, respectively. In this case, we say that they are *degenerate*.

We will exploit $|x\rangle$ to compute a superposition $|\chi_{0,1}\rangle \dots |\chi_{0,m-1}\rangle \dots |\chi_{i,j}\rangle \dots |\chi_{m-2,m-1}\rangle$, which we will denote for simplicity by $|\chi\rangle$. We interpret the values $\chi_{0,1}, \dots, \chi_{0,m-1}, \dots, \chi_{i,j}, \dots, \chi_{m-2,m-1}$ as the entries of a square binary matrix C , where $C[i][j] = \chi_{i,j}$ and whose entries along and below the main diagonal are undefined. We use such entries to represent the existence of crossings between pairs of edges in a graph drawing. Namely, $\chi_{i,j} = 1$ if e_i and e_j belong to E and cross, and $\chi_{i,j} = 0$ if either e_i and e_j belong to E and do not cross or at least one of e_i and e_j does not belong to E . Let χ be the string obtained by concatenating $\chi_{0,1}, \dots, \chi_{0,m-1}, \dots, \chi_{i,j}, \dots, \chi_{m-2,m-1}$. The values of χ are completely determined by x and by whether the considered layout is a book layout or a 2-level drawing. For every $0 \leq a < b \leq m-1$, consider the value $\chi_{a,b}$, where $e_a = (v_i, v_k)$ and $e_b = (v_j, v_\ell)$. In a book layout of G in which the vertex order is $\Pi(x)$, we have that $\chi_{a,b} = 1$ if e_a and e_b belong to E and cross (refer to the conditions in Fig. 32), and $\chi_{a,b} = 0$ if either e_a and e_b belong to E and do not cross or at least one of e_a and e_b does not belong to E . If $D(x)$ corresponds to a 2-level drawing of G , then we have that $\chi_{a,b} = 1$ if e_a and e_b belong to E and cross (i.e., $x_{i,j} \neq x_{k,\ell}$), and $\chi_{a,b} = 0$ if either e_a and e_b belong to E and do not cross (i.e., $x_{i,j} = x_{k,\ell}$) or at least one of e_a and e_b does not belong to E .

Recall that, the SKEWNESS TRASDUCER circuit outputs the superposition $|\theta\rangle |f(\theta)\rangle |e_0\rangle \dots |e_i\rangle \dots |e_{m-1}\rangle$ such that, when $f(\theta) = 1$, it holds that $e_i = 1$ if and only if there exists a $j \in [\sigma]$ such that $\theta[j]$ coincides with (the binary representation of) the integer i . In the following, for simplicity, we denote the superposition $|e_0\rangle \dots |e_i\rangle \dots |e_{m-1}\rangle$ as $|e\rangle$. Observe that, during the computation for problems TLS and BS, we manage the superposition $|\Theta\rangle = \sum_{\theta \in \mathbb{B}^{\sigma \log m}} c_\theta |\theta\rangle$, which includes all possible states corresponding to a selection of σ edges of G . Specifically, consider any basis state θ that appears in $|\Theta\rangle$, which represents a (multi)subset $N(\theta)$ of size σ of the set $[m]$. Recall that, the integers contained in θ are the labels of the edges of G . We denote by $K(\theta)$ the subset of the edges of G whose indices appear in $N(\theta)$. Observe that, if $N(\theta)$ does not contain repeated entries, then $K(\theta)$ is a subset of σ edges of G (with no repeated edges); this occurs exactly when $f(\theta) = 1$. If $N(\theta)$ contains repeated entries, then we say that it is *degenerate*.

6.1 Problem TLCM

We call TLCM the SOLUTION DETECTOR circuit for problem TLCM. Recall that, for the TLCM problem, we denote by ρ the maximum number of crossings allowed in the sought 2-level drawing of G .

Lemma 6.1. *There exists a gate TLCM that, when provided with the input superposition $|f(\phi)\rangle |x\rangle |0_h\rangle |-\rangle$, where $h = \frac{5m(m-1)}{2} - \log m - \log(m-1) - 2$, produces the output superposition $(-1)^{g(x)f(\phi)} |f(\phi)\rangle |x\rangle |0_h\rangle |-\rangle$, where $g(x) = 1$ if $D(x)$ is not degenerate and the 2-level drawing $D(x)$ of G has at most ρ crossings. TLCM has $O(m^2)$ circuit complexity, $O(n^2)$ depth, and $O(m^2)$ width.*

Proof of Lemma 6.1. Gate TLCM uses four gates: TL-CROSS FINDER U_χ , CROSS COUNTER U_{cc} , CROSS COMPARATOR $U_{c<}$, and FINAL CHECK U_{fc} , followed by the inverse gates $U_{c<}^{-1}$, U_{cc}^{-1} , and U_χ^{-1} . Refer to Fig. 12.

TL-CROSS FINDER. The purpose of U_χ is to compute the crossings in $D(x)$ (under the assumption that $D(x)$ is not degenerate), determined by the vertex order corresponding to x ; refer to Fig. 13b. When

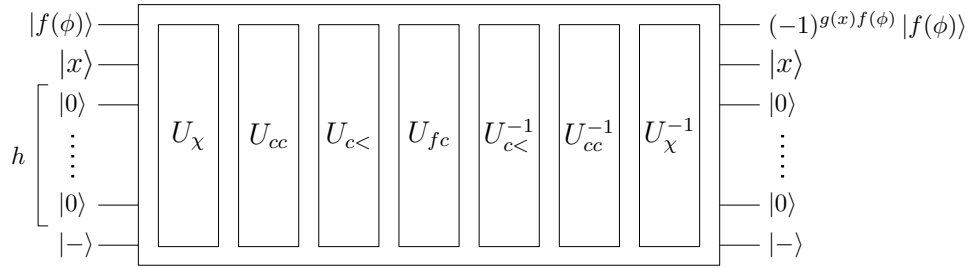


Figure 12: TLCM Oracle Pipeline.

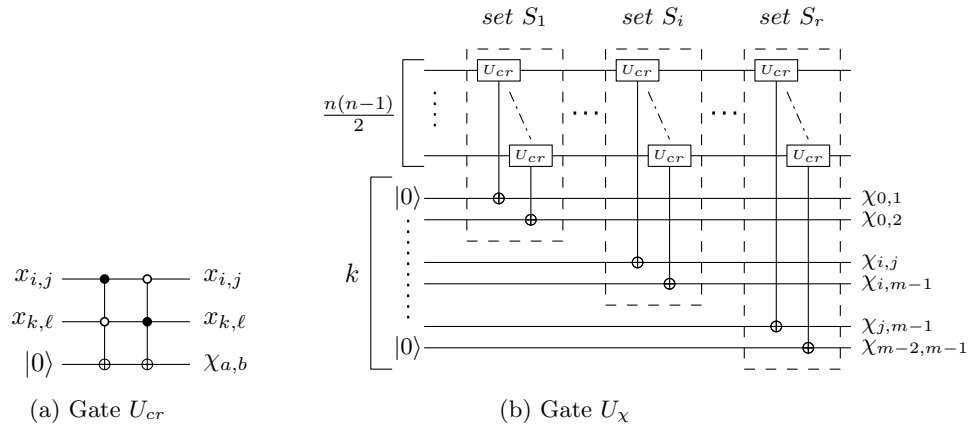


Figure 13: The gate U_{cr} (a) and gate U_χ (b). In (b), it holds $k = \frac{m(m-1)}{2}$.

provided with the input superposition $|x\rangle|0_k\rangle$, where $k = \frac{m(m-1)}{2}$, the gate U_x produces the output superposition $|x\rangle|\chi\rangle$.

The gate U_χ exploits the auxiliary gate U_{cr} , whose purpose is to check if two edges cross; refer to Fig. 13a. When provided with the input superposition $|x_{i,j}\rangle|x_{k,\ell}\rangle|0\rangle$, the gate produces the output superposition $|x_{i,j}\rangle|x_{k,\ell}\rangle|\chi_{a,b}\rangle$, where $e_a = (u_i, v_k)$, $e_b = (u_j, v_\ell)$, and $\chi_{a,b} = x_{i,j} \oplus x_{k,\ell}$ (which is 1 if and only if e_a and e_b cross in $D(x)$). It is implemented using two Toffoli gates with three inputs and outputs. The first one is activated when the qubit $|x_{i,j}\rangle$ is equal to $|1\rangle$ and the qubit $|x_{k,\ell}\rangle$ is equal to $|0\rangle$. The second one is activated when the qubit $|x_{i,j}\rangle$ is equal to $|0\rangle$ and the qubit $|x_{k,\ell}\rangle$ is equal to $|1\rangle$. U_{cr} has $O(1)$ circuit complexity, depth, and width.

The gate U_χ works as follows. Consider that if two variables $x_{i,j}$ and $x_{k,\ell}$ are compared to determine whether the edges (u_i, v_k) and (u_j, v_ℓ) cross, none of these variables can be compared with another variable at the same time. Therefore, we partition the pairs of such variables using Lemma 2.1 (with $k = 2$ and $|X| = \frac{n(n-1)}{2}$) into $r \in O(n^2)$ cross-independent sets S_1, \dots, S_r each containing at most $\frac{n(n-1)}{4}$ pairs. For $i = 1, \dots, r$, the gate U_χ executes in parallel a U_{cr} gate, for each pair $(x_{i,j}, x_{k,\ell})$ in S_i (refer to Fig. 13b), in order to output the qubit $|\chi_{a,b}\rangle$. U_χ has $O(n^4)$ circuit complexity, $O(n^2)$ depth, and $O(n^2)$ width.

CROSS COUNTER. The purpose of gate U_{cc} is to count the total number of crossings in the drawing $D(x)$. When provided with the input superposition $|\chi\rangle|0_h\rangle|0_k\rangle$, where $h = \log m + \log(m-1)$ and $k = 2m(m-1) - 2(\log m + \log(m-1)) - 2$, the gate U_{cc} produces the output superposition $|\chi\rangle|\sigma(x)\rangle|0_h\rangle$, where $\sigma(x) = \sum_{e_i, e_j \in E} \chi_{i,j}$ is a binary integer of length $\log m + \log(m-1)$ representing the total number of crossings. The gate U_{cc} is an instance of the gate U_{1s} (refer to Fig. 3), where the qubits of the superposition $|\chi\rangle = |\chi_{0,1}\rangle \dots |\chi_{0,m-1}\rangle \dots |\chi_{i,j}\rangle \dots |\chi_{m-2,m-1}\rangle$ play the role of the qubits of the superposition $|b_0 \dots b_{t-1}\rangle$, where $t = m$, which forms part of the input of U_{1s} . Observe that the number of crossings in $D(x)$ is at most $\frac{m(m-1)}{2}$. Therefore, the number $\sigma(x)$ of crossings in $D(x)$ can be represented by a binary string of length $h \leq \log m + \log(m-1)$. By Lemma 3.3, replacing $t = \frac{m(m-1)}{2}$, we get that the parameter $k = 2m(m-1) - 2(\log m + \log(m-1)) - 2$. By Lemma 3.3, gate U_{cc} has $O(m^2)$ circuit complexity, $O(\log^2 m)$ depth, and $O(m^2)$ width.

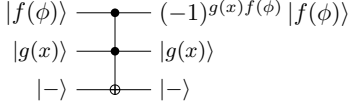


Figure 14: Gate U_{fc} .

CROSS COMPARATOR. The purpose of gate $U_{c<}$ is to verify if the total number of crossings $\sigma(x)$ in $D(x)$ computed by gate U_{cc} is less than the allowed number of crossings ρ . When provided with the input superposition $|\sigma(x)\rangle|\rho\rangle|0_h\rangle|0\rangle$, where $h = \log m + \log(m-1)$, the gate $U_{c<}$ produces the output superposition $|\sigma(x)\rangle|\rho\rangle|0_h\rangle|g(x)\rangle$, where $g(x) = 1$ if $D(x)$ is not degenerate and $\sigma(x) < \rho$. The gate $U_{c<}$ is an instance of the gate $U_{<}$ (refer to Fig. 2), where the $h = \log m + \log(m-1)$ qubits of the superposition $|\sigma(x)\rangle$ play the role of the qubits of the superposition $|\phi[i]\rangle$ and where h qubits initialized to the binary representation of ρ play the role of $|\phi[j]\rangle$. By Lemma 3.2, gate $U_{c<}$ has $O(\log m)$ circuit complexity, depth, and width.

FINAL CHECK. The purpose of gate U_{fc} is to check whether the current solution is admissible, i.e., whether the 2-level drawing $D(x)$ of G is not degenerate and it has at most ρ crossings. Refer to Fig. 14. When provided with the input superposition $|f(\phi)\rangle|g(x)\rangle|-\rangle$, the gate U_{fc} produces the outputs superposition $(-1)^{g(x)f(\phi)}|f(\phi)\rangle|g(x)\rangle|-\rangle$. U_{fc} exploits a Toffoli gate with three inputs and outputs. The control qubits are $|f(\phi)\rangle$ and $|g(x)\rangle$, and the target qubit is $|-\rangle$. When $f(\phi) = g(x) = 1$, the target qubit is transformed into the qubit $-|-\rangle$. Otherwise it leaves unchanged. Gate U_{fc} has $O(1)$ circuit complexity, depth, and width.

The inverse circuits. The purpose of circuits $U_{c<}^{-1}$, U_{cc}^{-1} , and U_{χ}^{-1} is to restore the h ancilla qubit to $|0\rangle$ so that they can be used in the subsequent steps of Grover's approach.

Correctness and complexity. For the correctness of Lemma 6.1, observe that the gates U_{χ} , U_{cc} , $U_{c<}$, and U_{fc} verify all the necessary conditions for which $D(x)$ has at most ρ crossings, under the assumption that $D(x)$ is not degenerate. Therefore, the sign of the output superposition of gate TLCM, which is determined by the expression $(-1)^{g(x)f(\phi)}$, is positive when either $D(x)$ is degenerate or $D(x)$ is not degenerate and the number of crossings $\sigma(x)$ in $D(x)$ is larger than ρ , and it is negative when $D(x)$ is not degenerate and the number of crossings $\sigma(x)$ in $D(x)$ is smaller than ρ . The bound on the circuit complexity descends from the circuit complexity of the gate U_{cc} , the bound on the depth descends from the depth of the gate U_{χ} , and the bound on the width descends from the width of U_{cc} . \square

6.2 Problem TLKP

We call TLKP the SOLUTION DETECTOR circuit for problem TLKP. Recall that, for TLKP problem, we denote by k the maximum number of crossings allowed for each edge in the sought 2-level drawing of G .

Lemma 6.2. *There exists a gate TLKP that, when provided with the input superposition $|f(\phi)\rangle|x\rangle|0_h\rangle|-\rangle$, where $h = \frac{m(m-1)}{2} + 4m - 2\log m - 4 + m(\log m + 1)$, outputs the superposition $(-1)^{g(x)f(\phi)}|f(\phi)\rangle|x\rangle|0_h\rangle|-\rangle$, where $g(x) = 1$ if $D(x)$ is not degenerate and each edge of the 2-level drawing $D(x)$ of G has at most k crossings. TLKP has $O(m^2)$ circuit complexity, $O(m \log^2 m)$ depth and $O(m)$ width.*

Proof of Lemma 6.2. Gate TLKP uses four gates: TL-CROSS FINDER U_{χ} , EDGE CROSS COUNTER U_{ecc} , EDGE CROSS COMPARATOR $U_{<k}$, and FINAL CHECK U_{fc} , followed by the inverse gates U_{χ}^{-1} , U_{ecc}^{-1} , and $U_{<k}^{-1}$. Refer to Fig. 15.

TL-CROSS FINDER. For the definition of gate U_{χ} , refer to the proof of Lemma 6.1. Recall that the purpose of U_{χ} is to compute the crossings in $D(x)$ (under the assumption that $D(x)$ is not degenerate), determined by the vertex order corresponding to x . Also recall that, when provided with the input superposition $|x\rangle|0_k\rangle$, the gate U_{χ} produces the output superposition $|x\rangle|\chi\rangle$.

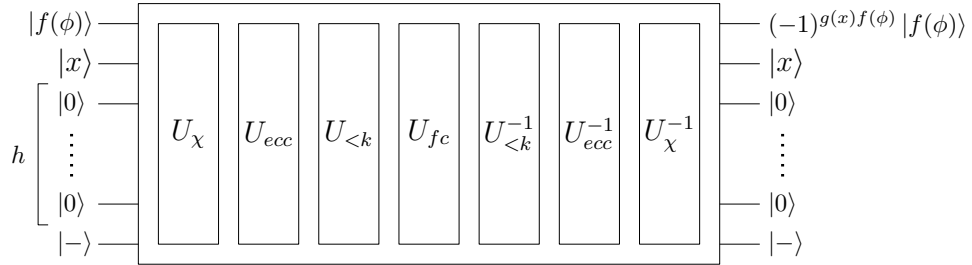


Figure 15: TLKP Oracle Pipeline.

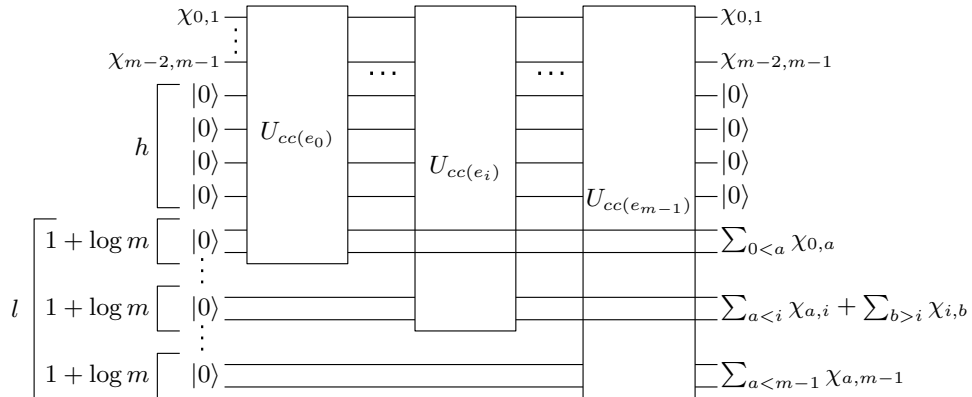


Figure 16: The gate U_{ecc} .

EDGE CROSS COUNTER. The purpose of gate U_{ecc} is to count, for each edge $e_i \in E$, the total number of crossings of each edge e_i in the drawing $D(x)$. When provided with the input superposition $|\chi\rangle|0_h\rangle|0_l\rangle$, where $h = 4m - 2\log m - 4$ and $l = m(1 + \log m)$, the gate U_{ecc} produces the output superposition $|\chi\rangle|0_h\rangle|\sigma_{e_0}(x)\rangle \dots |\sigma_{e_i}(x)\rangle \dots |\sigma_{e_{m-1}}(x)\rangle$, where $\sigma_{e_i}(x) = \sum_{a < i} \chi_{a,i} + \sum_{b > i} \chi_{i,b}$ is a binary integer of length $1 + \log m$ representing the total number of crossings of the edge e_i in $D(x)$. The gate U_{ecc} exploits the auxiliary gate $U_{cc(e_i)}$, whose purpose, for each edge e_i , is to compute the binary integer $\sigma_{e_i}(x)$. When provided with the input superposition $|\chi_{0,i}\rangle \dots |\chi_{i,i+1}\rangle \dots |\chi_{i,m-1}\rangle|0_h\rangle|0_{1+\log m}\rangle$, the gate $U_{cc(e_i)}$ produces the output superposition $|\chi_{0,i}\rangle \dots |\chi_{i,i+1}\rangle \dots |\chi_{i,m-1}\rangle|0_h\rangle|\sigma_{e_i}(x)\rangle$. The gate $U_{cc(e_i)}$ is an instance of the gate U_{1s} (refer to Fig. 3), where the qubits of the superposition $|\chi_{0,i}\rangle \dots |\chi_{i,i+1}\rangle \dots |\chi_{i,m-1}\rangle$ play the role of the qubits of the superposition $|b_0 \dots b_{t-1}\rangle$, with $t = m$, which forms part of the input of U_{1s} . Observe that, for each edge e_i , the number of crossings of e_i in $D(x)$ is at most $m - 1$. Therefore, $\sigma_{e_i}(x)$ can be represented by a binary string of length $1 + \log m$. By Lemma 3.3, gate $U_{cc(e_i)}$ has circuit complexity $O(m)$, depth complexity $O(\log^2 m)$, and width complexity $O(m)$. Gate U_{ecc} works as follows; refer to Fig. 16. Gate U_{ecc} executes in sequence gates $U_{cc(e_0)}$, $U_{cc(e_1)}$, \dots , $U_{cc(e_{m-1})}$. Gate U_{ecc} has circuit complexity $O(m^2)$, depth $O(m \log^2 m)$, and width $O(m)$.

EDGE CROSS COMPARATOR. The purpose of $U_{< k}$ is to verify, for each edge $e_i \in E$, if the total number of crossings $\sigma_{e_i}(x)$ of e_i in $D(x)$ computed by U_{ecc} is less than the allowed number of crossings for each edge k ; refer to Fig. 17. When provided with the input superposition $|\sigma_E(x)\rangle |k\rangle |0_h\rangle |0_m\rangle |0\rangle$, where $\sigma_E(x) = \sigma_{e_0}(x) \dots \sigma_{e_i}(x) \dots \sigma_{e_{m-1}}(x)$ and $h = \log m + 1$, the gate $U_{< k}$ produces the output superposition $|\sigma_E(x)\rangle |k\rangle |0_h\rangle |0_m\rangle |g(x)\rangle$, where $g(x) = 1$ if $D(x)$ is not degenerate and $\sigma_{e_i}(x) < k$ for each $e_i \in E$. The gate $U_{< k}$ exploits m instances of gate $U_<$ (refer to Fig. 2 and to Lemma 3.2), where the qubits of the superposition $|\sigma_{e_i}(x)\rangle$ play the role of the qubits of the superposition $|\phi[i]\rangle$ and the qubits initialized to the binary representation of k play the role of $|\phi[j]\rangle$. Recall that, by Lemma 3.2, gate $U_<$ has $O(\log m)$ circuit complexity, depth, and width. Each of the m gates $U_<$ provides an answer qubit ($|\kappa_i\rangle$), which is equal to 1 if and only if $\sigma_{e_i}(x) < k$ for the considered edge e_i . At the end of the m -th computation a Toffoli gate with $m + 1$ inputs and outputs is applied to check if, for each $e_i \in E$, $\sigma_{e_i}(x) < k$. Gate $U_{< k}$ has $O(m \log m)$ circuit complexity, $O(m \log m)$ depth, and $O(m)$ width.

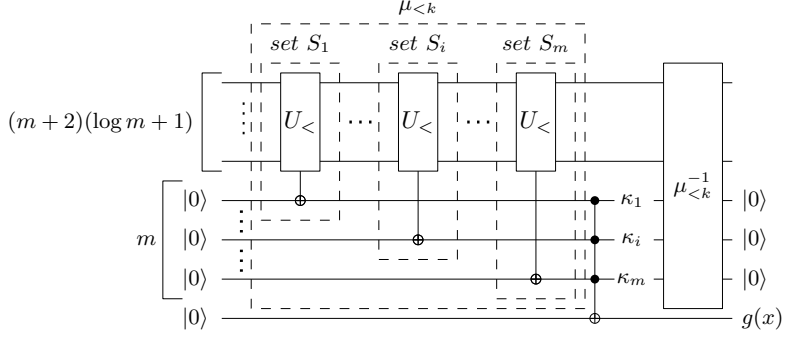


Figure 17: $U_{<k}$.

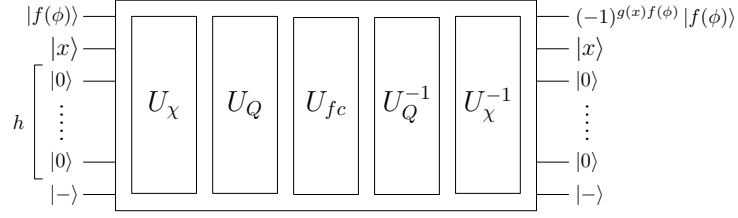


Figure 18: TLQP Oracle Pipeline.

FINAL CHECK. The purpose of gate U_{fc} is to check whether the current solution is admissible, i.e., whether the 2-level drawing $D(x)$ of G is not degenerate and each edge has at most k crossings. Refer to Fig. 14. When provided with the input superposition $|f(\phi)\rangle |g(x)\rangle |-\rangle$, the gate U_{fc} produces the outputs superposition $(-1)^{f(\phi)g(x)} |-\rangle$. U_{fc} exploits a Toffoli gate with three inputs and outputs. The control qubits are $|f(\phi)\rangle$ and $|g(x)\rangle$, and the target qubit is $|-\rangle$. When at least one of $f(\phi)$ and $g(x)$ are equal to 0, the target qubit leaves unchanged. On the other hand, when $f(\phi) = g(x) = 1$, the target qubit is transformed into the qubit $|-\rangle$. Gate U_{fc} has $O(1)$ circuit complexity, depth and width.

The inverse circuits. The purpose of circuits $U_{<k}^{-1}$, $U_{cc(E)}^{-1}$, and U_χ^{-1} is to restore the h ancilla qubit to $|0\rangle$ so that they can be used in the subsequent steps of Grover's approach.

Correctness and complexity. For the correctness of Lemma 6.2, observe that the gates U_χ , $U_{cc(E)}$, $U_{<k}$, and U_{fc} verify all the necessary conditions for which $D(x)$, for each edge of G , has at most k crossings, under the assumption that $D(x)$ is not degenerate. Therefore, the sign of the output superposition of gate TLKP, which is determined by the expression $(-1)^{g(x)f(\phi)}$, is positive when either $D(x)$ is degenerate or $D(x)$ is not degenerate and the number of crossings $\sigma_{e_i}(x)$ in $D(x)$ is larger than k , for some edge $e_i \in E$, and it is negative when $D(x)$ is not degenerate and the number of crossings $\sigma_{e_i}(x)$ in $D(x)$ is smaller than k , for each edge $e_i \in E$. The bounds on the circuit complexity, depth, and width descend from the circuit complexity, depth, and width of the gate $U_{cc(E)}$. \square

6.3 Problem TLQP

We call TLQP the SOLUTION DETECTOR circuit for problem TLQP.

Lemma 6.3. *There exists a gate TLQP that, when provided with the input superposition $|f(\phi)\rangle |x\rangle |0_h\rangle |-\rangle$, where $h \in O(m^4)$, produces the output superposition $(-1)^{f(\phi)g(x)} |f(\phi)\rangle |x\rangle |0_h\rangle |-\rangle$, and $g(x) = 1$ if $D(x)$ is not degenerate and the 2-level drawing $D(x)$ of G is quasi-planar. TLQP has $O(m^6)$ circuit complexity, $O(m^4)$ depth, and $O(m^2)$ width.*

Proof of Lemma 6.3. Gate TLQP executes three gates: TL-CROSS FINDER U_χ , QUASI-PLANARITY TESTER U_Q , and FINAL CHECK U_{fc} , followed by their inverse gates U_Q^{-1} and U_χ^{-1} . Refer to Fig. 18.

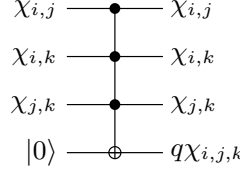


Figure 19: Gate $U_{q\chi}$

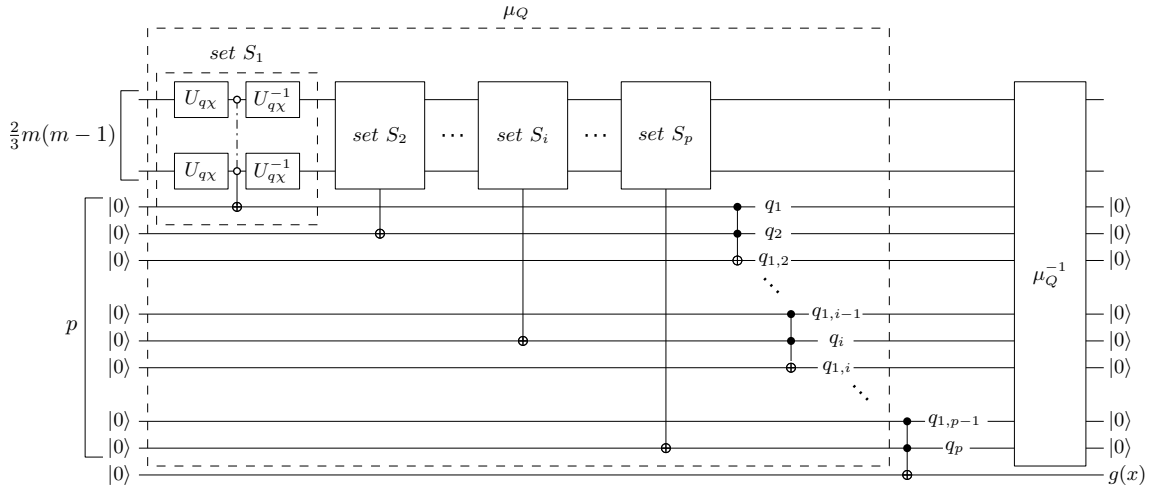


Figure 20: Gate U_Q

TL-CROSS FINDER. For the definition of gate U_χ , refer to the proof of Lemma 6.1. Recall that the purpose of U_χ is to compute the crossings in $D(x)$ (under the assumption that $D(x)$ is not degenerate), determined by the vertex order corresponding to x . Also recall that, when provided with the input superposition $|x\rangle|0_k\rangle$, the gate U_χ produces the output superposition $|x\rangle|\chi\rangle$.

QUASI-PLANARITY TESTER. The purpose of gate U_Q is to verify the absence of any three edges that pairwise cross in $D(x)$; refer to Fig. 20. When provided with the input the superposition $|\chi\rangle|0_h\rangle|0\rangle$, where $h \in O(m^4)$, the gate U_Q produces the output superposition $|\chi\rangle|0_h\rangle|g(x)\rangle$, where $g(x) = 1$ if $D(x)$ is not degenerate and there are not three edges that pairwise cross in $D(x)$.

The gate U_Q exploits the auxiliary gate $U_{q\chi}$, whose purpose is to check if three edges pairwise cross; refer to Fig. 19. When provided with the input superposition $|\chi_{i,j}\rangle|\chi_{i,k}\rangle|\chi_{j,k}\rangle|0\rangle$, the gate provide the output superposition $|\chi_{i,j}\rangle|\chi_{i,k}\rangle|\chi_{j,k}\rangle|q\chi_{i,j,k}\rangle$, where $q\chi_{i,j,k} = \chi_{i,j} \wedge \chi_{i,k} \wedge \chi_{j,k}$ (which is 1 if and only if e_i, e_j , and e_k pairwise cross in $D(x)$). It is implemented using a Toffoli gate with four inputs and outputs, which is activated when $\chi_{i,j} = \chi_{i,k} = \chi_{j,k} = 1$. The circuit complexity, depth, and width of $U_{q\chi}$ is $O(1)$.

The gate U_Q works as follows. Consider that if three variables $\chi_{i,j}, \chi_{i,k}$, and $\chi_{j,k}$ are compared to determine whether the edges e_i, e_j , and e_k pairwise cross, none of these variables can be compared with another variable at the same time. Therefore, we partition the pairs of such variables using Lemma 2.1 (with $k = 3$ and $|X| = \frac{m(m-1)}{2}$) into $p \in O(m^4)$ cross-independent sets S_1, \dots, S_p each containing at most $\frac{m(m-1)}{6}$ unordered triples. For $i = 1, \dots, p$, the gate U_Q executes in parallel a gate $U_{q\chi}$ for each triple $\{\chi_{i,j}, \chi_{i,k}, \chi_{j,k}\}$ in S_i (refer to Fig. 20). All the last output qubits of the $U_{q\chi}$ gates in S_i enter a Toffoli gate that outputs a qubit $|q_i\rangle$ such that $q_i = 1$ if and only if all of such qubits are equal to $|0\rangle$, i.e., it does not exist a triple of edges that pairwise cross. In order to allow the reuse of the ancilla qubit, except for the qubit $|q_i\rangle$, gate U_Q executes in parallel a gate $U_{q\chi}^{-1}$ for each triple in S_i . All the qubits $|q_i\rangle$, with $i = 1, \dots, p$, enter in cascade a Toffoli gate, with three inputs and outputs, that checks that all of them are equal to $|1\rangle$, i.e., there exist not three edges that pairwise cross. The output qubit of the last Toffoli gate is the qubit $|g(x)\rangle$. The gate U_Q has circuit complexity $O(m^6)$, $O(m^4)$ depth, and $O(m^2)$ width.

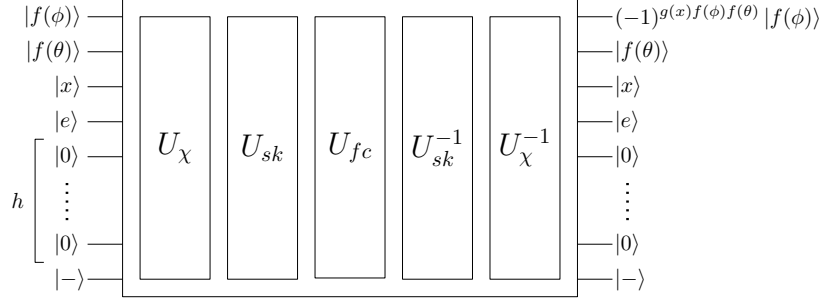


Figure 21: TLS Oracle Pipeline.

FINAL CHECK. We use a gate U_{fc} to check whether the current solution is admissible, i.e., whether the 2-level drawing $D(x)$ of G is not degenerate and the 2-level drawing $D(x)$ of G is quasi-planar. Refer to Fig. 14 and to Lemma 6.1. To this aim, we provide the U_{fc} with the qubit $|f(\phi)\rangle$, a qubit $|-\rangle$, and the qubit $|g(x)\rangle$ provided by gate U_Q . Recall that, gate U_{fc} has $O(1)$ circuit complexity, depth, and width.

The inverse circuits. The purpose of circuits U_Q^{-1} and U_χ^{-1} is to restore the h ancilla qubit to $|0\rangle$ so that they can be used in the subsequent steps of Grover's approach.

Correctness and complexity. For the correctness of Lemma 6.3, observe that the gates U_χ , U_Q , and U_{fc} verify all the necessary conditions for which $D(x)$ is a quasi-planar drawing of G , under the assumption that $D(x)$ is not degenerate. Therefore, the sign of the output superposition of gate TLQP, which is determined by the expression $(-1)^{g(x)f(\phi)}$, is positive when either $D(x)$ is degenerate or $D(x)$ is not degenerate and it is not a quasi-planar drawing of G , and it is negative when $D(x)$ is not degenerate and $D(x)$ is a quasi-planar drawing of G . The bounds on the circuit complexity, depth, and width descend from the circuit complexity, depth, and width of the gate U_Q . \square

6.4 Problem TLS

Recall that the purpose of the basis state $|0\rangle$ is to represent a subset $K(\theta)$ of the edges of G of size at most σ , each labeled with an integer in $[m]$, and that we denote by $N(\theta)$ the set of indices of the edges in $K(\theta)$. Also, recall that we denote by $D(x)$ the 2-level drawing of G associated with the vertex order corresponding to x . In the following, for a subgraph G' of G , we use the notation $D(x, G')$ to denote the 2-level drawing of G' induced by $D(x)$.

We call TLS the SOLUTION DETECTOR circuit for problem TLS.

Lemma 6.4. *There exists a gate TLS that, provided with the input superposition $|f(\phi)\rangle |f(\theta)\rangle |x\rangle |e\rangle |0_h\rangle |-\rangle$, where $h \in O(m^2)$, produces the output superposition $(-1)^{g(x)f(\phi)f(\theta)} |f(\phi)\rangle |f(\theta)\rangle |x\rangle |e\rangle |0_h\rangle |-\rangle$, such that, if $D(x)$ and $N(\theta)$ are not degenerate, then $g(x) = 1$ if and only if $D(x, G')$ is planar, where $G' = (V, E \setminus K(\theta))$. Gate TLS has $O(m^2)$ circuit complexity, $O(m)$ depth, and $O(m)$ width.*

Proof of Lemma 6.4. Gate TLS uses three gates: TL-CROSS FINDER U_χ , SKEWNESS CROSS TESTER U_{sk} , and FINAL CHECK U_{fc} , followed by the inverse gates U_{sk}^{-1} and U_χ^{-1} . Fig. 21

TL-CROSS FINDER. For the definition of gate U_χ , refer to the proof of Lemma 6.1. Recall that the purpose of U_χ is to compute the crossings in $D(x)$ (under the assumption that $D(x)$ is not degenerate), determined by the vertex order corresponding to x . Also recall that, when provided with the input superposition $|x\rangle |0_k\rangle$, the gate U_χ produces the output superposition $|x\rangle |\chi\rangle$.

SKEWNESS CROSS TESTER. Consider the subgraph G' of G obtained by removing from G all the edges in $K(\theta)$. The purpose of gate U_{sk} is to determine which of the crossings stored in $|\chi\rangle$ involve pairs of edges that are both absent from $|e\rangle$. In fact, all the edges not in $|e\rangle$ form the edge set of G' . Therefore, U_{sk} verifies whether the 2-layer drawing $D(x, G')$ of G' is planar; refer to Fig. 23. When provided with the input superposition $|\chi\rangle |e\rangle |0_{\frac{m}{2}+p}\rangle |0\rangle$, where $p \in O(m)$, the gate U_{sk} produces the output superposition $|\chi\rangle |e\rangle |0_{\frac{m}{2}+p}\rangle |g(x)\rangle$, such that, if $D(x)$ and $N(\theta)$ are not degenerate, then $g(x) = 1$ if and only if $D(x, G')$ is planar.

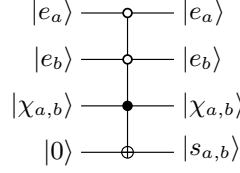


Figure 22: Gate U_k

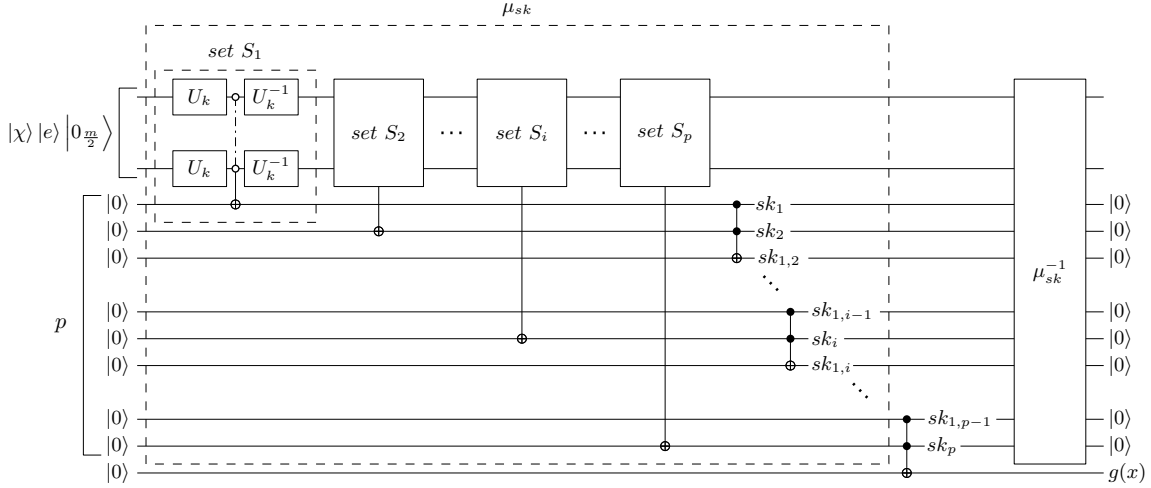


Figure 23: Gate U_{sk} .

The gate U_{sk} exploits the auxiliary gate U_k , whose purpose is to check if any two edges in G' cross; refer to Fig. 22. When provided with the input superposition $|e_a\rangle|e_b\rangle|\chi_{a,b}\rangle|0\rangle$, the gate U_k provides the output superposition $|e_a\rangle|e_b\rangle|\chi_{a,b}\rangle|s_{a,b}\rangle$, where $s_{a,b} = \neg e_a \wedge \neg e_b \wedge \chi_{a,b}$ (which is 1 if and only if e_a and e_b cross in $D(x, G')$). The gate U_k is implemented using a Toffoli gate with four inputs and outputs. The control qubits are $|e_a\rangle$, $|e_b\rangle$, and $|\chi_{a,b}\rangle$. The target qubit is set to $|0\rangle$. The gate is activated when $e_a = e_b = 0$ and $\chi_{a,b} = 1$. The circuit complexity, depth, and width of U_k is $O(1)$.

The gate U_{sk} works as follows. Consider that if two variables e_a and e_b are compared to determine whether the corresponding edges cross in $D(x, G')$, none of these variables can be compared with another variable at the same time. Therefore, we partition the pairs of such variables using Lemma 2.1 (with $k = 2$ and $|X| = m$) into $p \in O(m)$ cross-independent sets S_1, \dots, S_p each containing at most $\frac{m}{2}$ pairs. For $i = 1, \dots, p$, the gate U_{sk} executes in parallel a gate U_k , for each pair of variables e_a, e_b in S_i (together with the corresponding qubit $\chi_{a,b}$), in order to output the qubit $|\neg e_a \wedge \neg e_b \wedge \chi_{a,b}\rangle$. All the last output qubits of the U_k gates in S_i enter a Toffoli gate that outputs a qubit $|sk_i\rangle$ such that $sk_i = 1$ if and only if all of them are equal to $|0\rangle$, i.e., there exist no two crossing edges among the pairs in S_i . In order to allow the reuse of the ancilla qubit, except for the qubit $|sk_i\rangle$, gate U_{sk} executes in parallel a gate U_k^{-1} for each pair in S_i . To check if all qubits $|sk_i\rangle$ are equal to $|1\rangle$, for $i = 1, \dots, p$, we use a series of Toffoli gates T_i , each with three inputs and outputs. The first Toffoli gate T_1 receives in input the qubits $|sk_1\rangle$, $|sk_2\rangle$, and a qubit set to $|0\rangle$, and outputs the qubit $|sk_{1,2}\rangle = |sk_1 \wedge sk_2\rangle$. For $i = 2, \dots, p$, the Toffoli gate T_i receives in input the qubits $|sk_{1,i-1}\rangle$, $|sk_i\rangle$, and a qubit set to $|0\rangle$, and outputs the qubit $|sk_{1,i}\rangle = |sk_{1,i-1} \wedge sk_i\rangle$. The output qubit $|sk_{1,p}\rangle$ of the last Toffoli gate T_p is the qubit $|g(x)\rangle$. The gate U_{sk} has circuit complexity $O(m^2)$, depth $O(m)$, and width $O(m)$.

FINAL CHECK. The purpose of gate U_{fc} is to check whether the current solution is admissible, i.e., whether the 2-level drawing $D(x)$ and the set of indices $N(\theta)$ are both not degenerate and the 2-level drawing $D(x, G')$ of G' is planar. See Fig. 24. When provided with the input superposition $|f(\phi)\rangle|f(\theta)\rangle|g(x)\rangle|-\rangle$, the gate U_{fc} produces the outputs superposition $(-1)^{g(x)f(\phi)f(\theta)}|f(\phi)\rangle|f(\theta)\rangle|g(x)\rangle|-\rangle$. Gate U_{fc} exploits a Toffoli gate with four inputs and outputs. The control qubits are $|f(\phi)\rangle$, $|f(\theta)\rangle$, and $|g(x)\rangle$, and the target qubit is $|-\rangle$. When at least one of $f(\phi)$, $f(\theta)$, and $g(x)$ are equal to 0, the target qubit leaves

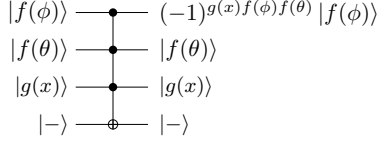


Figure 24: Gate U_{fc} .

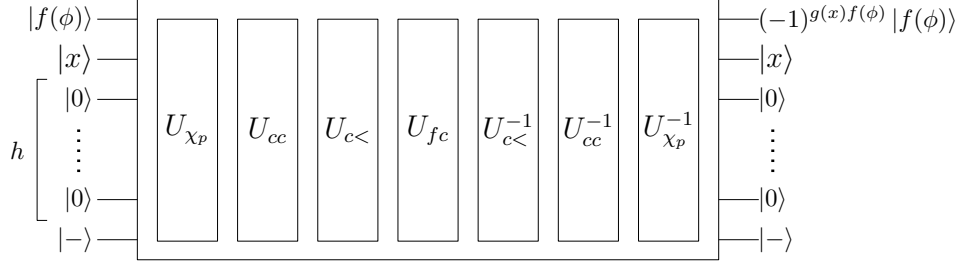


Figure 25: Oracle OPCM.

unchanged. On the other hand, when $f(\phi) = f(\theta) = g(x) = 1$, the target qubit is transformed into the qubit $−|−\rangle$. Gate U_{fc} has $O(1)$ circuit complexity, depth, and width.

The inverse circuits. The purpose of circuits U_{sk}^{-1} and U_{χ}^{-1} is to restore the h ancilla qubit to $|0\rangle$ so that they can be used in the subsequent steps of Grover’s approach.

Correctness and complexity. For the correctness of Lemma 6.4, observe that the gates U_{χ} , U_{sk} , and U_{fc} verify all the necessary conditions for which $D(x, G')$ is a 2-level planar drawing of G' , under the assumption that $D(x)$ and $N(\theta)$ are not degenerate. Therefore, the sign of the output superposition of gate TLS, which is determined by the expression $(−1)^{g(x)f(\phi)f(\theta)}$, is defined as follows. It is positive when either $D(x)$ or $N(\theta)$ are degenerate or $D(x)$ and $N(\theta)$ are not degenerate and the drawing $D(x, G')$ of G' is not planar. It is negative when $D(x)$ and $N(\theta)$ are not degenerate and the 2-level drawing $D(x, G')$ of G' is planar. The bounds on the circuit complexity, depth, and width of gate TLS descend from those of gate U_{sk} . \square

6.5 Problem OPCM

We call OPCM the SOLUTION DETECTOR circuit for problem OPCM. Recall that, for the OPCM problem, we denote by ρ the maximum number of crossings allowed in the sought 1-page layout of G . Also, recall that we denote by $\Pi(x)$ the vertex order along the spine of a book layout of G defined by the vertex order corresponding to x .

Lemma 6.5. *There exists a gate OPCM that, when provided with the input superposition $|f(\phi)\rangle|x\rangle|0_h\rangle|-\rangle$, where $h \in O(m^2)$, produces the output superposition $(−1)^{g(x,f(\phi))}|f(\phi)\rangle|x\rangle|0_h\rangle|-\rangle$, where $g(x) = 1$ if $\Pi(x)$ is not degenerate and the 1-page layout of G defined by $\Pi(x)$ has at most ρ crossings. OPCM has $O(n^8)$ circuit complexity, $O(n^6)$ depth, and $O(m^2)$ width.*

Proof of Lemma 6.5. Gate OPCM executes four gates: OP-CROSS FINDER U_{xp} , CROSS COUNTER U_{cc} , CROSS COMPARATOR $U_{c<}$, and FINAL CHECK U_{fc} , followed by the inverse gate U_{cc}^{-1} , $U_{c<}^{-1}$, and U_{xp}^{-1} . Refer to Fig. 25.

OP-CROSS FINDER. The purpose of U_{xp} is to compute the crossings in the 1-page layout of G defined by $\Pi(x)$, determined by the vertex order corresponding to x ; refer to Fig. 26. When provided with the input superposition $|x\rangle|0_k\rangle$, where $k = \frac{m(m-1)}{2}$, the gate U_{px} produces the output superposition $|x\rangle|\chi\rangle$.

The gate U_{xp} exploits the auxiliary gate U_{λ} , whose purpose is to check if two edges cross in the 1-page layout of G defined by $\Pi(x)$; refer to Fig. 26a. When provided with the input superposition $|x_{i,k}\rangle|x_{k,j}\rangle|x_{j,n}\rangle|x_{i,n}\rangle|0\rangle$, the gate U_{λ} produces the output superposition $|x_{i,k}\rangle|x_{k,j}\rangle|x_{j,n}\rangle|x_{i,n}\rangle|\chi_{a,b}\rangle$, where $e_a = (v_i, v_j)$, $e_b = (v_k, v_n)$, and $\chi_{a,b}$ equals 1 if and only if e_a and e_b cross in the 1-page layout of

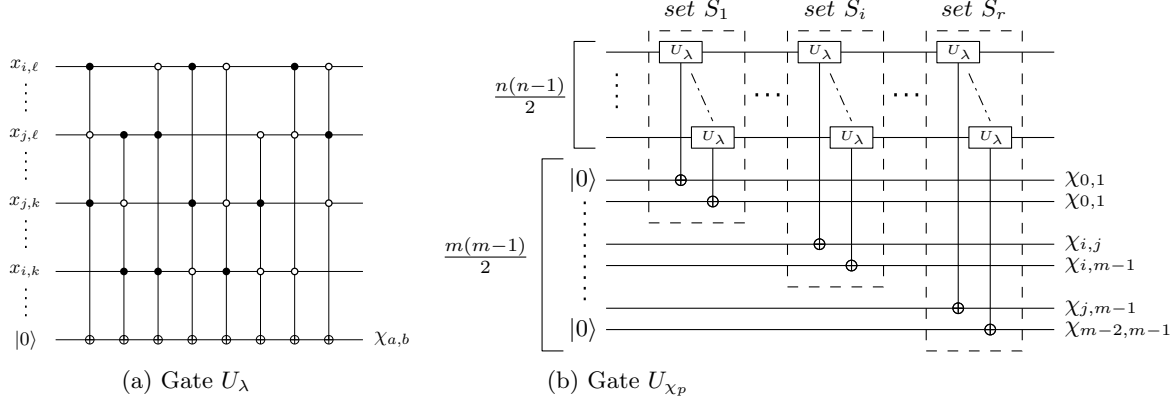


Figure 26: The gate U_λ (left) and gate U_{χ_p} (right).

G defined by $\Pi(x)$; refer to Fig. 32 and to the expression $\chi_{a,b}$ in Sect. 7.2. It is implemented using eight Toffoli gates, each with four inputs and outputs. In the following, we assume that $i < k < j < \ell$. The first is activated when $x_{i,\ell} = x_{j,k} = 1$ and $x_{j,\ell} = 0$ (see Fig. 32, top row, first column). The second is activated when $x_{i,k} = x_{j,\ell} = 1$ and $x_{j,k} = 0$ (see Fig. 32, top row, second column). The third is activated when $x_{j,\ell} = x_{i,k} = 1$ and $x_{i,\ell} = 0$ (see Fig. 32, top row, third column). The fourth is activated when $x_{j,k} = x_{i,\ell} = 1$ and $x_{i,k} = 0$ (see Fig. 32, top row, fourth column). The fifth is activated when $x_{i,k} = 1$ and $x_{i,\ell} = x_{j,k} = 0$ (see Fig. 32, second row, first column). The sixth is activated when $x_{j,k} = 1$ and $x_{j,\ell} = x_{i,k} = 0$ (see Fig. 32, second row, second column). The seventh is activated when $x_{i,\ell} = 1$ and $x_{i,k} = x_{j,\ell} = 0$ (see Fig. 32, second row, third column). The eighth is activated when $x_{j,\ell} = 1$ and $x_{j,k} = x_{i,\ell} = 0$ (see Fig. 32, second row, fourth column).

The gate U_{χ_p} works as follows. Consider that if four variables $x_{i,k}, x_{k,j}, x_{j,n}$ and $x_{i,n}$ are compared to determine whether the edges (v_i, v_j) and (v_k, v_n) cross, none of these variables can be compared with another variable at the same time. Therefore, we partition the pairs of such variables using Lemma 2.1 (with $k = 4$ and $|X| = \frac{n(n-1)}{2}$) into $r \in O(n^6)$ cross-independent sets s_1, \dots, S_r each containing at most $\frac{n(n-1)}{8}$ pairs. For $i = 1, \dots, r$, the gate U_{χ_p} executes in parallel a U_λ gate, for each quartet $(x_{i,k}, x_{k,j}, x_{j,n}, x_{i,n})$ in S_i (refer to Fig. 26b), in order to outputs the qubit $|\chi_{a,b}\rangle$. U_{χ_p} has circuit complexity $O(n^8)$, depth complexity $O(n^6)$ and width complexity $O(n^2)$.

CROSS COUNTER. The purpose of gate U_{cc} , as mention earlier, is to count the total number of crossings in the 1-page layout of G defined by $\Pi(x)$; refer to Fig. 3. Recall that, when provided with the input superposition $|\chi\rangle|0_h\rangle|0_k\rangle$, where $h = \log m + \log(m-1)$ and $k = 2m(m-1) - 2(\log m + \log(m-1)) - 1$, the gate U_{cc} produces the output superposition $|\chi\rangle|\sigma(x)\rangle|0_h\rangle$.

CROSS COMPARATOR. The purpose of gate $U_{c<}$, as mention earlier, is to verify if the total number of crossings $\sigma(x)$ in the 1-page layout of G defined by $\Pi(x)$ compute by the gate U_{cc} is less than the allowed number of crossings ρ ; refer to Fig. 2. Recall that, when provided with the input superposition $|\sigma(x)\rangle|\rho\rangle|0_h\rangle|0\rangle$, where $h = \log m + \log(m-1)$, the gate $U_{c<}$ produces the output superposition $|\sigma(x)\rangle|\rho\rangle|0_h\rangle|g(x)\rangle$, where $g(x) = 1$ if $\Pi(x)$ is not degenerate and $\sigma(x) < \rho$.

FINAL CHECK. The purpose of gate U_{fc} is to check whether the current solution is admissible, i.e., whether $\Pi(x)$ is not degenerate and the 1-page layout of G defined by $\Pi(x)$ has at most ρ crossings. Refer to Fig. 14. When provided with the input superposition $|f(\phi)\rangle|g(x)\rangle|-\rangle$, the gate U_{fc} produces the outputs superposition $(-1)^{g(x)f(\phi)}|f(\phi)\rangle|g(x)\rangle|-\rangle$. U_{fc} exploits a Toffoli gate with three inputs and outputs. The control qubits are $|f(\phi)\rangle$ and $|g(x)\rangle$, and the target qubit is $|-\rangle$. When at least one of $f(\phi)$ and $g(x)$ are equal to 0, the target qubit leaves unchanged. On the other hand, when $f(\phi) = g(x) = 1$, the target qubit is transformed into the qubit $|-\rangle$. Gate U_{fc} has $O(1)$ circuit complexity, depth, and width.

The inverse circuits. The purpose of circuits $U_{c<}^{-1}$, U_{cc}^{-1} , and U_χ^{-1} is to restore the h ancilla qubit to $|0\rangle$ so that they can be used in the subsequent steps of Grover's approach.

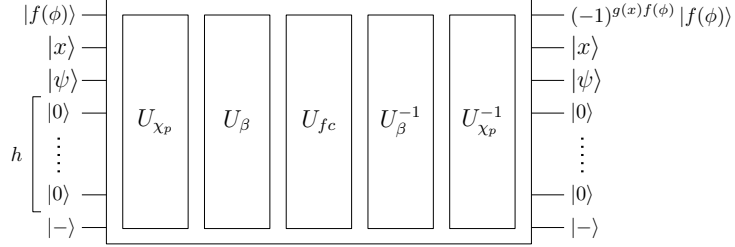


Figure 27: BT Oracle Pipeline.

Correctness and complexity. For the correctness of Lemma 6.5, observe that the gates $U_{χ}$, U_{cc} , $U_{c<}$, and U_{fc} verify all the necessary conditions for which the 1-page layout of G defined by $\Pi(x)$ has at most $ρ$ crossings, under the assumption that $\Pi(x)$ is not degenerate. Therefore, the sign of the output superposition of gate OPCM, which is determined by the expression $(-1)^{g(x)f(ϕ)}$, is positive when either $\Pi(x)$ is degenerate or $\Pi(x)$ is not degenerate and the number of crossings $σ(x)$ in the 1-page layout of G defined by $\Pi(x)$ is larger than $ρ$, and it is negative only if $\Pi(x)$ is not degenerate and the number of crossings $σ(x)$ in the 1-page layout of G defined by $\Pi(x)$ is smaller than $ρ$. The bound on the circuit complexity descends from the circuit complexity of the gate $U_{χ_p}$, the bound on the depth descends from the depth of the gate $U_{χ_p}$, and the bound on the width descends from the width of U_{cc} . $□$

6.6 Problem BT

We call BT the SOLUTION DETECTOR circuit for problem BT. Recall that, for the BT problem, we denote by $τ$ the number of pages allowed in the sought book layout drawing of G .

Recall that, during the computation, we manage the superposition $|\Psi\rangle = \sum_{\psi \in \mathbb{B}^{m \log \tau}} c_\psi |\psi\rangle$ whose purpose is to represent a coloring of the edges of G with colors in the set $[\tau]$. Specifically, consider any basis state ψ that appears in $|\Psi\rangle$. We denote by $P(\psi)$ the page assignment of the edges of G to $τ$ pages in which, for $i = 0, \dots, m - 1$, the edge e_i is assigned to the page $\psi[i]$.

Lemma 6.6. *There exists a gate BT that, when provided with the input superposition $|f(ϕ)\rangle |\psi\rangle |x\rangle |0_h\rangle |-\rangle$, where $h \in O(m^2)$, produces the output superposition $(-1)^{g(x,\psi)f(ϕ)} |f(ϕ)\rangle |\psi\rangle |x\rangle |0_h\rangle |-\rangle$, where $g(x,\psi) = 1$ if $\Pi(x)$ is not degenerate and there exists a book layout of G on $τ$ pages in which the vertex order is $\Pi(x)$ and the page assignment is $P(\psi)$. Gate BT has $O(n^8)$ circuit complexity, $O(n^6)$ depth, and $O(m)$ width.*

Proof of Lemma 6.6. Gate BT uses two gates: OP-CROSS FINDER $U_{χ_p}$, COLOR TESTER $U_β$, and FINAL CHECK U_{fc} , followed by the inverse gates $U_β^{-1}$ and $U_{χ_p}^{-1}$. Refer to Fig. 27.

OP-CROSS FINDER. For the definition of gate $U_{χ_p}$, refer to the proof of Lemma 6.5. Recall that the purpose of $U_{χ_p}$ is to compute the crossings in the 1-page layout of G defined by $\Pi(x)$, determined by the vertex order corresponding to x . Also recall that, when provided with the input superposition $|x\rangle |0_k\rangle$, the gate U_{px} produces the output superposition $|x\rangle |\chi\rangle$.

COLOR TESTER. Consider the book layout $D(x, \psi)$ of G defined by the vertex order $\Pi(x)$ and the page assignment is $P(\psi)$. The purpose of gate $U_β$ is to verify if $D(x, \psi)$ is a book embedding of G on $τ$ pages, provided that $\Pi(x)$ is not degenerate; refer to Fig. 29. When provided with the input superposition $|\psi\rangle |\chi\rangle |0_b\rangle |0_r\rangle |0\rangle$, where $b = \frac{m}{2}(2 + \log \tau)$ and $r = m - 1$, the gate $U_β$ produces the output superposition $|\psi\rangle |\chi\rangle |0_b\rangle |0_r\rangle |g(x, \psi)\rangle$, where $g(x, \psi) = 1$ if $\Pi(x)$ is not degenerate and $D(x, \psi)$ is a book embedding of G on $τ$ pages.

The gate $U_β$ exploits the auxiliary gate $U_{=λ}$, whose purpose is to check if two edges that cross have the same color; refer to Fig. 28. When provided with the input superposition

$$|\psi[a][0]\rangle \dots |\psi[a][\log(\tau) - 1]\rangle |\psi[b][0]\rangle \dots |\psi[a][\log(\tau) - 1]\rangle |0_{\log \tau}\rangle |0\rangle |\chi_{a,b}\rangle |0\rangle ,$$

the gate produces the output superposition

$$|\psi[a][0]\rangle \dots |\psi[a][\log(\tau) - 1]\rangle |\psi[b][0]\rangle \dots |\psi[a][\log(\tau) - 1]\rangle |0_{\log \tau}\rangle |\psi[a] = \psi[b]\rangle |\chi_{a,b}\rangle |\chi_{a,b} \wedge (\psi[a] = \psi[b])\rangle .$$

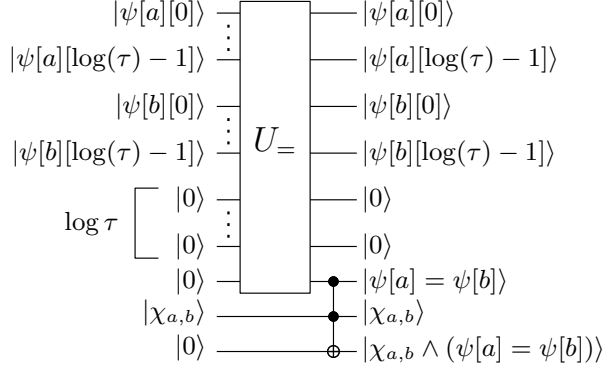


Figure 28: Gate $U_{=λ}$.

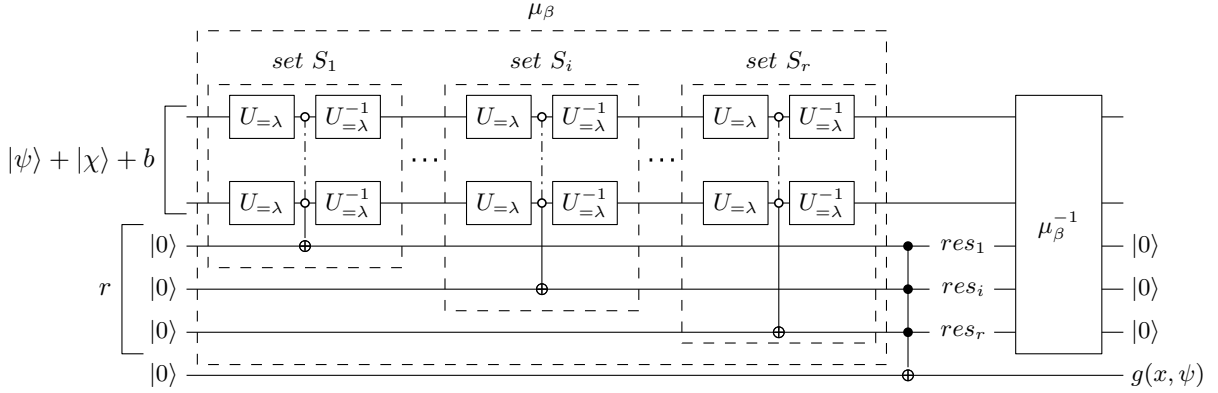


Figure 29: Gate $U_β$.

Gate $U_{=λ}$ exploits the auxiliary gates $U_=_$ to compare $ψ[a]$ and $ψ[b]$, and a Toffoli gate with two inputs and outputs to verify if edges e_a and e_b cross and have the same color. By Lemma 3.1, gate $U_{=λ}$ has $O(\log τ)$ circuit complexity, depth, and width.

The gate $U_β$ works as follows. Consider that if two variables $ψ[a]$ and $ψ[b]$ are compared to determine whether e_a and e_b have been assigned the same color, none of these variables can be compared with another variable at the same time. Therefore, we partition the pairs of such variables using Lemma 2.1 (with $k = 2$ and $|X| = m$) into $r \in O(m)$ cross-independent sets S_1, \dots, S_r each containing at most $\frac{m}{2}$ pairs. For $i = 1, \dots, r$, the gate $U_β$ executes in parallel a gate $U_{=λ}$, for each pair of variables $\{ψ[a], ψ[b]\} \in S_i$ (together with their corresponding qubit $χ_{a,b}$), in order to output the qubit $|χ_{a,b} \wedge (ψ[a] = ψ[b])⟩$. All the last output qubits of the $U_{=λ}$ gates for S_i enter a Toffoli gate that outputs a qubit $|res_i⟩$ such that $res_i = 1$ if and only if all of them are equal to $|0⟩$, i.e., it does not exist two crossing edges with the same color (among the pairs in S_i). In order to allow the reuse of the ancilla qubits, except for the qubit $|res_i⟩$, gate $U_β$ executes in parallel a gate $U_{=λ}^{-1}$ for each pair in S_i . All the qubits $|res_i⟩$ enter a Toffoli gate that outputs a qubit $|g(x, ψ)⟩$ such that $g(x, ψ) = 1$ if and only if all of them are equal to $|1⟩$, i.e., there exist no two edges of G with the same color that cross in $D(x, ψ)$. Gate $U_β$ has circuit complexity $O(m^2 \log τ)$, depth $O(m \log τ)$, and width $O(m)$.

FINAL CHECK. The purpose of gate U_{fc} is to check whether the current solution is admissible, i.e., whether $D(x, ψ)$ is a book embedding of G on $τ$ pages. Refer to Fig. 30. When provided with the input superposition $|f(ϕ)⟩ |g(x, ψ)⟩ |−⟩$, the gate U_{fc} produces the output superposition $(−1)^{g(x, ψ)f(ϕ)} |f(ϕ)⟩ |g(x, ψ)⟩ |−⟩$. Gate U_{fc} exploits a Toffoli gate with three inputs and outputs. The control qubits are $|f(ϕ)⟩$ and $|g(x, ψ)⟩$, and the target qubit is $|−⟩$. When at least one of $f(ϕ)$ and $g(x, ψ)$ are equal to 0, the target qubit leaves unchanged. On the other hand, when $f(ϕ) = g(x, ψ) = 1$, the target qubit is transformed into the qubit $−|−⟩$. Gate U_{fc} has $O(1)$ circuit complexity, depth, and width.

The inverse circuits. The purpose of circuits $U_β^{-1}$, and $U_{χ_p}^{-1}$ is to restore the h ancilla qubit to $|0⟩$ so that they can be used in the subsequent steps of Grover's approach.

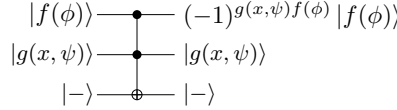


Figure 30: Gate U_{fc} .

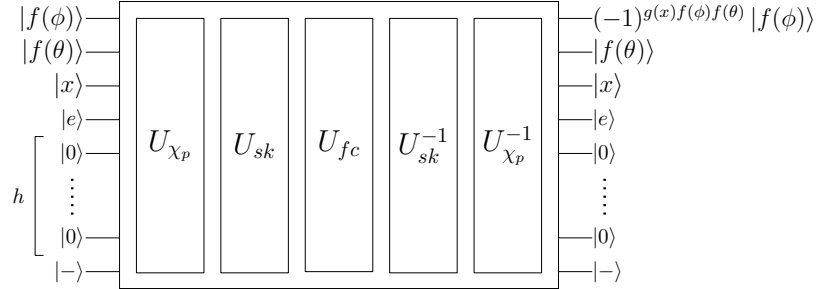


Figure 31: Oracle BS.

Correctness and complexity. For the correctness of Lemma 6.6, observe that the gates U_{χ_p} and U_{β} verify all the necessary conditions for which $D(x, \psi)$ is a book embedding of G with τ pages, under the assumption that $\Pi(x)$ is not degenerate. Therefore, the sign of the output superposition of gate BT, which is determined by the expression $(-1)^{g(x,\psi)f(\phi)}$, is positive when either $\Pi(x)$ is degenerate or $\Pi(x)$ is not degenerate and the book layout $D(x, \psi)$ is not a book embedding of G with τ pages, and it is negative only if $\Pi(x)$ is not degenerate and $D(x, \psi)$ is a book embedding of G with τ pages. The bound on the circuit complexity descends from the circuit complexity of gate U_{χ_p} , the bound on the depth descends from the depth of gate U_{χ_p} , and the bound on the width descends from the width of gate U_{β} . \square

6.7 Problem BS

We call BS the SOLUTION DETECTOR circuit for problem BS.

Lemma 6.7. *There exists a gate BS that, provided with the input superposition $|f(\phi)\rangle |f(\theta)\rangle |x\rangle |e\rangle |0_h\rangle |-\rangle$, where $h \in O(m^2)$, produces the output superposition $(-1)^{g(x)f(\phi)f(\theta)} |f(\phi)\rangle |f(\theta)\rangle |x\rangle |e\rangle |0_h\rangle |-\rangle$, such that, if $\Pi(x)$ and $N(\theta)$ are not degenerate, then $g(x) = 1$ if and only if the 1-page layout of G' determined by $\Pi(x)$ is a 1-page book embedding, where $G' = (V, E \setminus K(\theta))$. Gate BS has $O(n^8)$ circuit complexity, $O(n^6)$ depth, and $O(m)$ width.*

Proof of Lemma 6.7. Gate BS uses three gates: OP-CROSS FINDER U_{χ_p} , SKEWNESS CROSS TESTER U_{sk} , and FINAL CHECK U_{fc} , followed by the inverse gates U_{sk}^{-1} and $U_{\chi_p}^{-1}$. Refer to Fig. 31.

OP-CROSS FINDER. For the definition of gate U_{χ_p} , refer to the proof of Lemma 6.5. Recall that the purpose of U_{χ_p} is to compute the crossings in the 1-page layout of G defined by $\Pi(x)$, determined by the vertex order corresponding to x . Also recall that, when provided with the input superposition $|x\rangle |0_k\rangle$, the gate U_{χ_p} produces the output superposition $|x\rangle |\chi\rangle$.

SKEWNESS CROSS TESTER. For the definition of U_{sk} , refer to the proof of Lemma 6.4. Consider the subgraph G' of G obtained by removing from G all the edges in $K(\theta)$. The purpose of gate U_{sk} is to determine which of the crossings stored in $|\chi\rangle$ involve pairs of edges that are both absent from $|e\rangle$. In fact, all the edges not in $|e\rangle$ form the edge set of G' . Therefore, U_{sk} verifies whether the 1-page layout of G' determined by $\Pi(x)$ is a 1-page book embedding. When provided with the input superposition $|\chi\rangle |e\rangle |0_{\frac{m}{2}+p}\rangle |0\rangle$, where $p \in O(m)$, the gate U_{sk} produces the output superposition $|\chi\rangle |e\rangle |0_{\frac{m}{2}+p}\rangle |g(x)\rangle$, such that, if $\Pi(x)$ and $N(\theta)$ are not degenerate, then $g(x) = 1$ if and only the 1-page layout of G' determined by $\Pi(x)$ is a 1-page book embedding.

FINAL CHECK. For the definition of U_{fc} , refer to the proof of Lemma 6.4. The purpose of gate U_{fc} is to check whether the current solution is admissible, i.e., whether the 1-page layout of G determined by $\Pi(x)$ and the set of indices $N(\theta)$ are both not degenerate and the 1-page layout of G' determined by $\Pi(x)$ is a 1-page book embedding. See Fig. 24. When provided with the input superposition $|f(\phi)\rangle|f(\theta)\rangle|g(x)\rangle|-\rangle$, the gate U_{fc} produces the outputs superposition $(-1)^{g(x)f(\phi)f(\theta)}|f(\phi)\rangle|f(\theta)\rangle|g(x)\rangle|-\rangle$.

The inverse circuits. The purpose of circuits U_{sk}^{-1} , and $U_{\chi_p}^{-1}$ is to restore the h ancilla qubit to $|0\rangle$ so that they can be used in the subsequent steps of Grover's approach.

Correctness and complexity. For the correctness of Lemma 6.7, observe that the gates U_{χ_p} , U_{sk} , and U_{fc} verify all the necessary conditions for which the 1-page layout of G' determined by $\Pi(x)$ is a 1-page book embedding, under the assumption that $\Pi(x)$ and $N(\theta)$ are not degenerate. Therefore, the sign of the output superposition of gate BS, which is determined by the expression $(-1)^{g(x)f(\phi)f(\theta)}$, is defined as follows. It is positive when either $\Pi(x)$ or $N(\theta)$ are degenerate or $\Pi(x)$ and $N(\theta)$ are not degenerate and the 1-page layout of G' determined by $\Pi(x)$ is a 1-page book embedding. It is negative when $\Pi(x)$ and $N(\theta)$ are not degenerate and the 1-page layout of G' determined by $\Pi(x)$ is a 1-page book embedding. The bounds on the circuit complexity and depth of gate BS descend from those of U_{χ_p} , whereas the bound on the width of BS descends from U_{sk} . \square

7 Exploiting Quantum Annealing for Graph Drawing

In this section, we explore the 2-level problems and the book layout problems, that we have addressed so far from the quantum circuit model perspective, in the context of the quantum annealing model of computation. We pragmatically concentrate on the D-Wave platform, which offers quantum annealing services based on large-scale quantum annealing solver. To utilize the hybrid facility of D-Wave for solving an optimization problem, there are essentially two ways: Either the problem is provided with its QUBO formulation or it is provided with a CBO formulation with constraints that are at most quadratic. Also, given a CBO formulation, it is quite simple to construct a QUBO formulation. Hence, in Sects. 7.1 and 7.2, we first provide CBO formulations for the problems introduced in the previous section. Second, we overview (Sect. 7.3) a standard method for transforming a CBO formulation into a QUBO formulation. Third, in Sect. 7.4, we discuss a detailed experiment conducted on the quantum annealing services provided by D-Wave, specifically focusing on TLCM, which has extensive experimental literature compared to other problems considered in this paper. These experiments evaluate the efficiency of D-Wave with respect to well-known classical approaches to the TLCM problem.

7.1 CBO Formulations for Two-Level Problems

Let $G = (U, V, E)$ be a bipartite graph. We denote by u_i , for $i = 1, \dots, |U|$, and v_j , for $j = |U| + 1, \dots, |U| + |V|$, the vertices in U and V , respectively. We start by describing the variables and the constraints needed to model the vertex ordering in a 2-level drawing, which are common to the formulations of TLCM, TLKP, TLQP, and TLS.

Ordering variables. To model the order of the vertices in U and V in a 2-level drawing Γ of G , we use $|U| \cdot (|U| - 1)$ binary variables $u_{i,j}$ for each ordered pair of vertices $u_i, u_j \in U$ and $|V| \cdot (|V| - 1)$ binary variables $v_{i,j}$ for each ordered pair of vertices $v_i, v_j \in V$. The variable $x_{i,j}$ is equal to 1 if and only if x_i precedes x_j in Γ , with $x \in \{u, v\}$.

Ordering constraints. We define the following constraints. As in [16], to model the fact that an assignment of values to the variables $x_{i,j}$, with $x \in \{u, v\}$, correctly models a linear ordering of the vertices in U and in V , we exploit two types of constraints:

CONSISTENCY: For each ordered pair of vertices $u_i, u_j \in U$, we have the constraint **(CU)** $u_{i,j} + u_{j,i} = 1$. Similarly, for each ordered pair of vertices $v_i, v_j \in V$, we have the constraint **(CV)** $v_{i,j} + v_{j,i} = 1$. Clearly, there exist $O(|U|^2)$ and $O(|V|^2)$ constraints of type **(CU)** and **(CV)**, respectively.

TRANSITIVITY: For each ordered triple of vertices $u_i, u_j, u_k \in U$, we have the constraints **(TU)** $u_{i,j} + u_{j,k} - u_{i,k} \geq 0$ and $u_{i,j} + u_{j,k} - u_{i,k} \leq 1$. The constraint **(TV)** for each ordered triple of vertices of V is defined analogously. Clearly, there exist $O(|U|^3)$ and $O(|V|^3)$ constraints of type **(TU)** and **(TV)**, respectively. Constraints **(TU)** and **(TV)** are linear. We also consider alternative quadratic constraints for transitivity: for each ordered triple of vertices $u_i, u_j, u_k \in U$, we have the constraints

(TQU) $1 - (u_{i,j} \cdot u_{j,k}) + u_{i,k} \geq 1$. The constraints (TQV) for each ordered triple of vertices of V are defined analogously. Clearly, the number of (TQU) and (TQV) constraints is half the number of (TU) and (TV) constraints.

Next, we provide specific variables and constraints that allow us to correctly model the problems TLCM, TLKP, TLQP, and TLS. To this aim, for each pair of independent edges $e_a = (u_i, v_k)$ and $e_b = (u_j, v_\ell)$, we define the expression $\chi_{a,b} = u_{i,j} \cdot v_{\ell,k} + u_{j,i} \cdot v_{k,\ell}$, which is equal to 1 if and only if e_a and e_b cross. For each edge $e \in E$, we denote by $I(e)$ the set of edges in E that do not share an endpoint with e .

Two-level Crossing Minimization (TLCM). We consider the minimization version of the problem. In order to minimize the total number of crossings in the sought 2-level drawing of G , we define the objective function (OF)

$$\min \sum_{e_a \in E} \sum_{e_b \in I(e_a)} \chi_{a,b}.$$

Two-level k -planarity (TLKP). We show how to model the fact that at most k crossings are allowed on each edge. We have the single constraint (KP)

$$\sum_{e_b \in I(e_a)} \chi_{a,b} \leq k.$$

Clearly, over all the edges of G , there are $|E|$ constraints of type (KP).

Two-level Quasi Planarity (TLQP). We show how to model the fact that no three edges are allowed to pairwise cross. For each ordered triple (e_a, e_b, e_c) of edges of E such that $e_b \in I(e_a)$ and $e_c \in I(e_a) \cap I(e_b)$, we have the constraint (QP)

$$\chi_{a,b} + \chi_{b,c} + \chi_{a,c} < 3.$$

Clearly, over all the edges of G , there are $O(|E|^3)$ constraints of type (QP).

Two-level Skewness (TLS). To model the membership of the edges to a subset S such that $|S| \leq \sigma$, whose removal from G yields a forest of caterpillars, we use $|E|$ binary variables $s_{i,j}$ for each edge (u_i, v_j) . The variable $s_{i,j}$ is equal to 1 if and only if (u_i, v_j) belongs to S . First, to enforce that $|S| \leq \sigma$, we use the constraint (CS)

$$\sum_{(u_i, v_j) \in E} s_{i,j} \leq \sigma.$$

Second, we show how to model the fact that no two edges in $E \setminus S$ are allowed to cross. For each edge $e_a = (u_i, v_j) \in E$ and for each edge $e_b = (u_\ell, v_k) \in I(e_a)$, we have the constraint (S)

$$\chi_{a,b} - s_{i,j} - s_{\ell,k} < 1.$$

Over all the edges of G there are $O(|E|^2)$ constraints of type (S).

7.2 CBO Formulations for Book-layout problems

Let $G = (V, E)$ be a graph. We denote by v_i , for $i = 1, \dots, |V|$, the vertices in V . As in Sect. 7.1, we use the variable $x_{i,j}$ to encode the precedence between the ordered pair of vertices $v_i, v_j \in V$. Moreover, in order for an assignment of values in \mathbb{B} to such variables to correctly model a linear ordering of V , we use the *consistency* and *transitivity* constraints described in Sect. 7.1.

Next, we provide the specific variables and constraints that allow us to correctly model the problems OPCM, BT, and BS. Two edges are *independent* if they do not share an end-vertex. To this aim, for each ordered pair of independent edges $e_a = (v_i, v_j)$ and $e_b = (v_\ell, v_k)$, we define the expression $\chi_{a,b} = x_{i,\ell} \cdot x_{\ell,j} \cdot x_{j,k} + x_{i,k} \cdot x_{k,j} \cdot x_{j,\ell} + x_{j,\ell} \cdot x_{\ell,i} \cdot x_{i,k} + x_{j,k} \cdot x_{k,i} \cdot x_{i,\ell}$, which is equal to 1 if and only if e_a and e_b cross and (exactly) one of the endpoints of e_a precedes both the endpoints of e_b ; refer to Fig. 32(top). More specifically, let $x_{\alpha,\beta} \cdot x_{\beta,\gamma} \cdot x_{\gamma,\delta}$ be any of the four terms that define $\chi_{a,b}$. We have that such a term evaluates to 1 if and only if the vertices $v_\alpha, v_\beta, v_\gamma$, and v_δ appear in this left-to-right order along the spine.

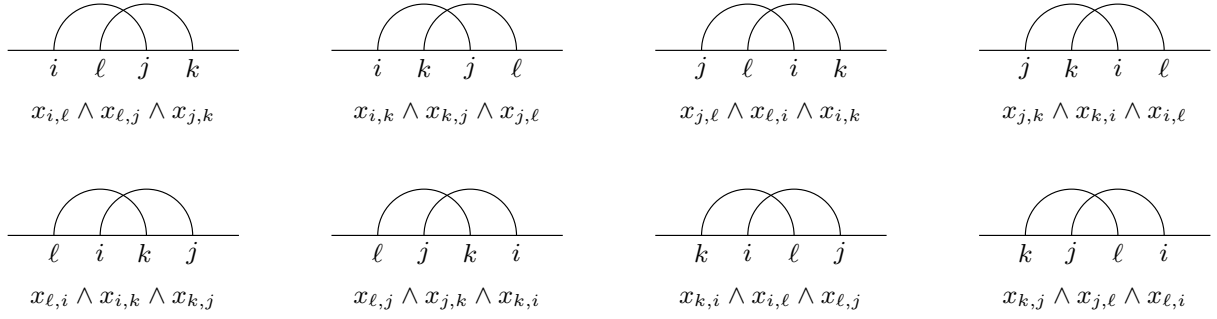


Figure 32: (top) The four possible crossing configurations of the edges $e_a = (v_i, v_j)$ and $e_b = (v_\ell, v_k)$, in which an end-vertex of e_a precedes both endpoints of e_b . (bottom) The four possible crossing configurations of the edges e_a and e_b , in which an end-vertex of e_b precedes both endpoints of e_a .

One-Page Crossing Minimization (OPCM). We consider the minimization version of the problem. In order to minimize the total number of crossings in the sought 1-page layout of G , we define the objective function **(OF)**

$$\min \sum_{e_a \in E} \sum_{e_b \in I(e_a)} \chi_{a,b}.$$

Book Thickness (BT). To model the membership of the edges to one of the τ pages, we use $\tau|E|$ binary variables $e_{i,j,c}$, for each edge (v_i, v_j) and for each page $c \in [\tau]$. The variable $e_{i,j,c}$ is equal to 1 if and only if (v_i, v_j) is assigned to page c . First, in order to enforce that each edge belongs exactly to one page, for each edge $(v_i, v_j) \in E$, we use the constraint **(BC)**

$$\sum_{c \in [\tau]} e_{i,j,c} = 1.$$

Second, we show how to model the fact that no two edges assigned to the same page are allowed to cross. For each edge $e_a = (v_i, v_j) \in E$, for each edge $e_b = (v_\ell, v_k) \in I(e_a)$, and for each page $c \in [\tau]$, we have the constraint **(CC)**

$$\chi_{a,b} + e_{i,j,c} + e_{\ell,k,c} < 3.$$

Book Skewness (BS). For this problem, we adopt the same constraints **(CS)** as for the TLS problem. Moreover, we adopt the constraints **(S)** as for the TLS problem.

7.3 From CBO to QUBO

The formulations presented in Sects. 7.1 and 7.2 contain quadratic and even cubic constraints. Such constraints, however, only involve binary variables. Hence, they can be easily linearized, by means of standard operations research techniques, to be exploited to define a QUBO formulation suitable for quantum annealing.

Specifically, let $\mu = \prod_{i=1}^k x_i$ be a (non-necessarily quadratic) monomial of total degree k , such that each variable x_i is a binary variable. We obtain an equivalent constraint by replacing each occurrence of μ in all the constraints of our formulation with a new binary variable z_μ and by adding the following $k+1$ constraints:

$$\begin{cases} z_\mu \leq x_i & i = 1, \dots, k \\ z_\mu \geq 1 - k + \sum_{i=1}^k x_i \end{cases}$$

In our formulation for the 2-level problems, the maximum degree of all monomials is 2 and these monomials arise from the expressions $\chi_{a,b}$, for each pair of independent edges $e_a = (u_i, v_i)$ and $e_b = (u_\ell, v_k)$. Thus, there exist at most $|E(G)|^2$ distinct degree-2 monomials in these formulations. Therefore, by applying the replacement described above, we introduce at most $|E(G)|^2$ new variables and $3|E(G)|^2$ new constraints. Similarly, in our formulation for the book layout problems, the maximum degree of all monomials is 3 and these monomials arise from the expressions $\chi_{a,b}$, for each pair of independent edges

$e_a = (u_i, v_i)$ and $e_b = (u_\ell, v_k)$. Thus, there exist at most $|E(G)|^2$ distinct degree-3 monomials in these formulations. Therefore, by applying the replacement described above, we introduce at most $|E(G)|^2$ new variables and $4|E(G)|^2$ new constraints.

Once the constraints are linearized, a QUBO formulation is obtained by inserting all constraints in the objective function. Note that if the problem is not an optimization problem an objective function is anyway created such that its optimum value is equal to zero. Constraints are first transformed so that their right member is equal to zero. For inequalities an extra variable is inserted so to transform the inequality into an equality. Then left member is squared and the result is inserted into the objective function.

7.4 D-Wave Experimentation

We performed our experiments on TLCM using the hybrid solver of D-Wave, which suitably mixes quantum computations with classic tabu-search and simulated annealing heuristics. The obtained results are not guaranteed to be optimal.

The D-Wave hybrid solver receives in input either a CBO or a QUBO formulation of a problem. We used it with a linear CBO formulation (with **(TU)** and **(TV)** constraints) and with a quadratic CBO formulation (with **(TQU)** and **(TQV)** constraints). Roughly, D-Wave hybrid solver works as follows. First, it decomposes the problem into parts that fit the quantum processor. The decomposition aims at selecting subsets of variables, and hence sub-problems, maximally contributing to the problem energy. Second, it solves such sub-problems with the quantum processor. Third, it injects the obtained results into the original overall problem that is solved with traditional heuristics. These steps can be repeated several times, since an intermediate solution can re-determine the set of variables that contribute the most to the energy of the problem. An interesting description of the behaviour and of the limitations of D-Wave is presented in [15], although it refers to the quantum processor called Chimera that has been replaced by the new processors called Pegasus and Zephyr.

We compare our results with the figures proposed in [6]. Namely, the authors compare three exact algorithms for TLCM: LIN, which is the standard linearization approach; JM, which is the algorithm in [16]; and SDP, which is the branch-and-bound in [22]. Their experiments were carried out on an Intel Xeon processor with 2.33 GHZ.

Table 2 illustrates the results of the experimentation we conducted on the D-Wave platform. We focused on the same set of graphs used in [6]. Namely, for each value of n , i.e., number of vertices per layer, and for each value of d , i.e., density, we performed 10 experiments on 10 distinct graph instances. Table 2 reports for each pair n, d the averages over such instances. The columns report what follows. *Best Current Time*: the best performance among the exact algorithms for TLCM known so far (time measured by [6]). *Approach*: one of LIN, JM, and SDP depending on which is the fastest approach. The double slash indicates that an optimal solution has not been found. *D-wave Time (Linear)*: time of our experiments, using the linear formulation. *# of Constraints (Linear)*: number of constraints of our linear formulation. *Crossings (Linear)*: number of crossings obtained with our linear formulation. *D-wave Time (Quadratic)*: time of our experiments, using the quadratic formulation. *# of Constraints (Quadratic)*: number of constraints of our quadratic formulation. *Crossings (Quadratic)*: number of crossings obtained with our quadratic formulation.

It is important to observe that the number of crossings we obtained was the optimal one for all graphs with 10 vertices per layer [30] (graphs above the horizontal line of Table 2). Unfortunately, the literature [6] does not report the actual minimum number of crossings for the remaining instances.

The comparison of the time employed by D-Wave (linear and quadratic) with the one of the best exact methods is quite promising, even if the times in the *Best Current Time* column are the results of a computation performed on a non-up-to-date classical hardware, and indicate that D-Wave can be used to efficiently tackle instances of TLCM. The comparison between linear and quadratic CBO formulations indicates that the quadratic formulation is more efficient, since it generates fewer constraints. Their behaviour in terms of number of crossings are quite similar. The time we report is the overall time elapsed between the remote call from our client and the reception of the result. The actual time spent on the quantum processor is always between 0.016 and 0.032 sec.

8 Conclusions and Open Problems

We initiate the study of quantum algorithms in the Graph Drawing research area, providing a framework that allows us to tackle several classic problems within the 2-level and book layout drawing standards. Our

Table 2: TLCM: D-Wave vs other approaches. Bipartite graphs with increasing number of vertices per layer and density. All times are in seconds.

n	d	Best Current Time	Approach	D-Wave Time (Linear)	# of Constraints (Linear)	Crossings (Linear)	D-Wave Time (Quadratic)	# of Constraints (Quadratic)	Crossings (Quadratic)
10	10	0,01	LIN	0,26	509	1	0,15	269	1
10	20	0,05	JM	0,92	1926	11	0,50	996	11
10	30	0,15	JM	1,48	2969	52	0,79	1529	52
10	40	0,33	JM	1,39	2970	142	0,76	1530	142
10	50	0,61	JM	1,44	2970	276	0,83	1530	276
10	60	1,14	JM	1,52	2970	259	0,81	1530	459
10	70	2,35	JM	1,47	2970	717	0,79	1530	717
10	80	4,05	JM	1,49	2970	1037	0,81	1530	1037
10	90	6,79	SDP	1,92	2970	1387	0,81	1530	1387
12	10	0,02	LIN	1,18	2293	0,67	0,61	1183	0,67
12	20	1,52	JM	2,15	4110	34,22	1,07	2110	34,22
12	30	4,53	JM	2,77	5263	139,11	1,41	2696	139,11
12	40	16,36	JM	2,72	5337	339,89	1,44	2734	339,89
12	50	44,84	SDP	2,80	5412	664,56	1,52	2772	664,56
12	60	48,26	SDP	2,94	5412	1040	1,44	2772	1040
12	70	40,31	SDP	2,71	5412	1535	1,48	2772	1535
12	80	28,71	SDP	2,82	5412	2228,67	1,63	2772	2228,56
12	90	22,21	SDP	2,88	5412	3023,67	1,68	2772	3023,67
14	10	0,33	LIN	2,30	3912	2,67	1,10	2008	2,67
14	20	89,61	SDP	4,19	7701	89,33	2,37	3933	89,33
14	30	132,72	SDP	4,69	8512	316,89	2,55	4344	316,78
14	40	144,03	SDP	5,20	8918	716	2,74	4550	716
14	50	180,49	SDP	4,71	8918	1316,11	2,88	4550	1316
14	60	141,93	SDP	4,67	8918	2053	2,35	4550	2052,89
14	70	149,68	SDP	4,93	8918	3017,78	2,76	4550	3016,22
14	80	145,97	SDP	5,03	8918	4258,89	2,46	4550	4257,67
14	90	81,27	SDP	4,92	8918	5865,33	2,39	4550	5875,22
16	10	2,77	LIN	3,45	6672	11,56	1,83	3410	11,56
16	20	309,31	SDP	6,70	12423	176,78	3,34	6324	176,33
16	30	630,31	SDP	7,53	13397	604,78	3,63	6817	603,89
16	40	800,87	SDP	7,56	13680	1326,89	3,73	6960	1324,44
16	50	451,09	SDP	7,46	13680	2376,89	3,82	6960	2375,44
16	60	403,82	SDP	7,33	13680	3770,11	3,73	6960	3762,67
16	70	789,62	SDP	7,48	13680	5501,67	3,77	6960	5486,78
16	80	568,55	SDP	7,37	13680	7591,78	3,66	6960	7575,11
16	90	362,29	SDP	7,08	13680	10336,11	3,72	6960	10310,89
18	10	7,06	LIN	6,16	12154	18,11	3,36	6187	18,11
18	20	778,86	SDP	10,25	18424	312,78	4,99	9358	309,56
20	10	117,72	LIN	10,25	19357	44,78	5,26	9828	44,33
20	20	1813,87	SDP	14,25	26589	551,33	7,34	13479	548,22
22	10	546,71	LIN	14,06	25942	94,22	7,09	13152	92,22
22	20	3443,81	SDP	19,62	35217	984,22	10,04	17830	962,44
24	10	2225,82	LIN	20,96	37757	150,44	10,69	19110	148,33
24	20	//	//	27,70	48788	1794,22	14,17	24669	1835,11

framework, equipped with several quantum circuits of potential interest to the community, builds upon Grover’s quantum search approach. It empowers us to achieve, at least, a quadratic speedup compared to the best classical exact algorithms for all the problems under consideration. In addition, we conducted experiments using the D-Wave quantum annealing platform for the TWO-LEVEL CROSSING MINIMIZATION problem. Our experiments demonstrated that the platform is highly suitable for addressing graph drawing problems and showcased significant efficiency when compared to the top approaches available for solving such problems. The encounter between Graph Drawing and Quantum Computing is still in its nascent stage, offering a vast array of new and promising problems. Virtually, all graph drawing problems can be explored through the lenses of quantum computation, utilizing both the quantum circuit model and, more pragmatically, quantum annealing platforms.

References

- [1] Aaronson, S.: Introduction to quantum information science lecture notes (April 2019), <https://www.scottaaronson.com/qclec.pdf>
- [2] Angelini, P., Da Lozzo, G., Di Battista, G., Frati, F., Patrignani, M.: 2-level quasi-planarity or how caterpillars climb (spqr-)trees. In: Marx, D. (ed.) Proceedings of the 2021 ACM-SIAM Symposium on Discrete Algorithms, SODA 2021, Virtual Conference, January 10 - 13, 2021. pp. 2779–2798. SIAM (2021). <https://doi.org/10.1137/1.9781611976465.165>
- [3] Angelini, P., Da Lozzo, G., Förster, H., Schneek, T.: 2-Layer k-Planar Graphs Density, Crossing Lemma, Relationships And Pathwidth. The Computer Journal (04 2023). <https://doi.org/10.1093/comjnl/bxad038>, <https://doi.org/10.1093/comjnl/bxad038>, bxad038
- [4] Bannister, M.J., Eppstein, D.: Crossing minimization for 1-page and 2-page drawings of graphs with bounded treewidth. *J. Graph Algorithms Appl.* **22**(4), 577–606 (2018). <https://doi.org/10.7155/jgaa.00479>, <https://doi.org/10.7155/jgaa.00479>
- [5] Bernhart, F., Kainen, P.C.: The book thickness of a graph. *J. Comb. Theory, Ser. B* **27**(3), 320–331 (1979). [https://doi.org/10.1016/0095-8956\(79\)90021-2](https://doi.org/10.1016/0095-8956(79)90021-2), [https://doi.org/10.1016/0095-8956\(79\)90021-2](https://doi.org/10.1016/0095-8956(79)90021-2)
- [6] Buchheim, C., Wiegele, A., Zheng, L.: Exact algorithms for the quadratic linear ordering problem. *INFORMS J. Comput.* **22**(1), 168–177 (2010). <https://doi.org/10.1287/ijoc.1090.0318>, <https://doi.org/10.1287/ijoc.1090.0318>
- [7] Courcelle, B.: The monadic second-order logic of graphs. i. recognizable sets of finite graphs. *Inf. Comput.* **85**(1), 12–75 (1990). [https://doi.org/10.1016/0890-5401\(90\)90043-H](https://doi.org/10.1016/0890-5401(90)90043-H), [https://doi.org/10.1016/0890-5401\(90\)90043-H](https://doi.org/10.1016/0890-5401(90)90043-H)
- [8] Courcelle, B., Engelfriet, J.: Graph Structure and Monadic Second-Order Logic - A Language-Theoretic Approach, Encyclopedia of mathematics and its applications, vol. 138. Cambridge University Press (2012), http://www.cambridge.org/fr/knowledge/item5758776/?site_locale=fr_FR
- [9] Di Battista, G., Eades, P., Tamassia, R., Tollis, I.G.: Graph Drawing: Algorithms for the Visualization of Graphs. Prentice-Hall (1999)
- [10] Dujmovic, V., Fellows, M.R., Kitching, M., Liotta, G., McCartin, C., Nishimura, N., Ragde, P., Rosamond, F.A., Whitesides, S., Wood, D.R.: On the parameterized complexity of layered graph drawing. *Algorithmica* **52**(2), 267–292 (2008). <https://doi.org/10.1007/s00453-007-9151-1>, <https://doi.org/10.1007/s00453-007-9151-1>
- [11] Eades, P., McKay, B.D., Wormald, N.C.: On an edge crossing problem. In: 9th Australian Computer Science Conference, ACSC 1986, Proceedings. pp. 327–334 (1986)
- [12] Eades, P., Wormald, N.C.: Edge crossings in drawings of bipartite graphs. *Algorithmica* **11**(4), 379–403 (1994). <https://doi.org/10.1007/BF01187020>, <https://doi.org/10.1007/BF01187020>
- [13] Garey, M.R., Johnson, D.S.: Crossing number is np-complete. *SIAM Journal on Algebraic Discrete Methods* **4**(3), 312–316 (1983). <https://doi.org/10.1137/0604033>, <https://doi.org/10.1137/0604033>
- [14] Grover, L.K.: A fast quantum mechanical algorithm for database search. In: Miller, G.L. (ed.) Proceedings of the Twenty-Eighth Annual ACM Symposium on the Theory of Computing, Philadelphia, Pennsylvania, USA, May 22-24, 1996. pp. 212–219. ACM (1996). <https://doi.org/10.1145/237814.237866>, <https://doi.org/10.1145/237814.237866>
- [15] Jünger, M., Lobe, E., Mutzel, P., Reinelt, G., Rendl, F., Rinaldi, G., Stollenwerk, T.: Performance of a quantum annealer for ising ground state computations on chimera graphs. *CoRR* **abs/1904.11965** (2019), <http://arxiv.org/abs/1904.11965>
- [16] Jünger, M., Mutzel, P.: 2-layer straightline crossing minimization: Performance of exact and heuristic algorithms. *J. Graph Algorithms Appl.* **1**(1), 1–25 (1997). <https://doi.org/10.7155/jgaa.00001>, <https://doi.org/10.7155/jgaa.00001>

- [17] Kobayashi, Y., Maruta, H., Nakae, Y., Tamaki, H.: A linear edge kernel for two-layer crossing minimization. *Theor. Comput. Sci.* **554**, 74–81 (2014). <https://doi.org/10.1016/j.tcs.2014.06.009>
- [18] Kobayashi, Y., Tamaki, H.: A faster fixed parameter algorithm for two-layer crossing minimization. *Inf. Process. Lett.* **116**(9), 547–549 (2016). <https://doi.org/10.1016/j.ipl.2016.04.012>
- [19] Masuda, S., Kashiwabara, T., Nakajima, K., Fujisawa, T.: On the np-completeness of a computer network layout problem. In: Proc. IEEE International Symposium on Circuits and Systems (ISCAS 1987). p. 292–295 (1987)
- [20] McGeoch, C.C.: Adiabatic Quantum Computation and Quantum Annealing: Theory and Practice. *Synthesis Lectures on Quantum Computing*, Morgan & Claypool Publishers (2014). <https://doi.org/10.2200/S00585ED1V01Y201407QMC008>
- [21] Nielsen, M.A., Chuang, I.L.: *Quantum Computation and Quantum Information* (10th Anniversary edition). Cambridge University Press (2016), <https://www.cambridge.org/de/academic/subjects/physics/quantum-physics-quantum-information-and-quantum-computation/quantum-computation-and-quantum-information-10th-anniversary-edition?format=HB>
- [22] Rendl, F., Rinaldi, G., Wiegele, A.: A branch and bound algorithm for max-cut based on combining semidefinite and polyhedral relaxations. In: Fischetti, M., Williamson, D.P. (eds.) *Integer Programming and Combinatorial Optimization*, 12th International IPCO Conference, Ithaca, NY, USA, June 25–27, 2007, Proceedings. Lecture Notes in Computer Science, vol. 4513, pp. 295–309. Springer (2007). https://doi.org/10.1007/978-3-540-72792-7_23
- [23] Rieffel, E., Polak, W.: *Quantum Computing: A Gentle Introduction*. The MIT Press, 1st edn. (2011)
- [24] Shahrokhi, F., Sýkora, O., Székely, L.A., Vrto, I.: Book embeddings and crossing numbers. In: Mayr, E.W., Schmidt, G., Tinhofer, G. (eds.) *Graph-Theoretic Concepts in Computer Science*, 20th International Workshop, WG '94, Herrsching, Germany, June 16–18, 1994, Proceedings. Lecture Notes in Computer Science, vol. 903, pp. 256–268. Springer (1994). https://doi.org/10.1007/3-540-59071-4_53
- [25] Tamassia, R. (ed.): *Handbook on Graph Drawing and Visualization*. Chapman and Hall/CRC (2013), <https://www.crcpress.com/Handbook-of-Graph-Drawing-and-Visualization/Tamassia/9781584884125>
- [26] Tan, J., Zhang, L.: The consecutive ones submatrix problem for sparse matrices. *Algorithmica* **48**(3), 287–299 (2007). <https://doi.org/10.1007/s00453-007-0118-z>, <https://doi.org/10.1007/s00453-007-0118-z>
- [27] Vizing, V.G.: On an estimate of the chromatic class of a p -graph. *Diskret. Analiz* (3), 25–30 (1964), <https://mathscinet.ams.org/mathscinet-getitem?mr=0180505>
- [28] Wigderson, A.: The complexity of the Hamiltonian circuit problem for maximal planar graphs. Tech. Rep. TR-298, Princeton University (1982)
- [29] Yannakakis, M.: Edge-deletion problems. *SIAM J. Comput.* **10**(2), 297–309 (1981). <https://doi.org/10.1137/0210021>, <https://doi.org/10.1137/0210021>
- [30] Zheng, L., Buchheim, C.: A new exact algorithm for the two-sided crossing minimization problem. In: *International Conference on Combinatorial Optimization and Applications* (2007)